

A New Approach to User Scheduling in Massive Multi-User MIMO Broadcast Channels

Gilwon Lee, *Student Member, IEEE* and Youngchul Sung[†], *Senior Member, IEEE*

Abstract

In this paper, a new user-scheduling-and-beamforming method is proposed for multi-user massive multiple-input multiple-output (massive MIMO) broadcast channels in the context of two-stage beamforming. The key ideas of the proposed scheduling method are 1) to use a set of *orthogonal reference* beams and construct a *double cone* around each reference beam to select ‘nearly-optimal’ semi-orthogonal users based only on channel quality indicator (CQI) feedback and 2) to apply *post-user-selection beam refinement* with zero-forcing beamforming (ZFBB) based on channel state information (CSI) feedback only from the selected users. It is proved that the proposed scheduling-and-beamforming method is asymptotically optimal as the number of users increases. Furthermore, the proposed scheduling-and-beamforming method almost achieves the performance of the existing semi-orthogonal user selection with ZFBB (SUS-ZFBB) that requires full CSI feedback from all users, with significantly reduced feedback overhead which is even less than that required by random beamforming.

Index Terms

User scheduling, multi-user MIMO, massive MIMO, two-stage beamforming, multi-user diversity, zero-forcing beamforming

[†] Corresponding author

Gilwon Lee and Youngchul Sung are with Dept. of Electrical Engineering, KAIST, Daejeon, 305-701, South Korea. E-mail: {gwlee@ and ysung@ee}.kaist.ac.kr. This research was supported by Basic Science Research Program through the National Research Foundation of Korea (NRF) funded by the Ministry of Education (2013R1A1A2A10060852). A preliminary version of this work was submitted to 2014 SPAWC [1].

I. INTRODUCTION

The multi-user multiple-input and multiple-output (MU-MIMO) technology has served as one of the core technologies of the fourth generation (4G) wireless systems. With the current interest in large-scale antenna arrays at base stations (BSs), the importance of the MU-MIMO technology further increases for future wireless systems. The MU-MIMO technology supports users in the same frequency band and time simultaneously based on spatial-division multiplexing, exploiting the degrees-of-freedom (DoF) in the spatial domain. There has been extensive research on MU-MIMO ranging from transmit signal or beamformer design to user scheduling in the past decade [2]–[5]. It is known that the capacity of a Gaussian MIMO broadcast channel is achieved by dirty paper coding (DPC) [2], [3], [6]. However, due to the difficulty of practical implementation of DPC, linear beamforming schemes for transmit signal design for MU-MIMO have become dominant in current cellular standards [7]. In general, linear beamforming schemes such as zero-forcing beamforming (ZFBF) and minimum mean-square-error (MMSE) beamforming perform worse than DPC. However, an astonishing remedy was brought to these linear beamforming schemes for MU-MIMO downlink, based on multi-user diversity [4], [5], [8], [9]. That is, with proper user selection or scheduling, the performance degradation of the linear beamforming schemes compared to DPC is negligible as the number of users in the served cell becomes large [4], [5], and the seminal results in [4], [5] have provided guidance on how to select simultaneous users in practical MU-MIMO downlink systems.

In this paper, we revisit the user scheduling and beamforming problem for MU-MIMO downlink in the context of up-to-date massive MU-MIMO downlink with two-stage beamforming [10], although the proposed user scheduling method can readily be applied to conventional single-stage MU-MIMO downlink. User scheduling for MU-MIMO cellular downlink has been investigated extensively in the past decade [4], [5], [11], [12]. Among many proposed user scheduling methods for beamforming-based MU-MIMO downlink are two well-known user selection schemes already mentioned in the above sitting on opposite sides on the scale of feedback overhead: random (orthogonal) beamforming (RBF) [4] and semi-orthogonal user selection with ZFBF (SUS-ZFBF) [5]. Both schemes are asymptotically optimal, i.e., the sum-rate scaling law with respect to (w.r.t.) the number of users in the cell is the same as that of DPC-based MU-MIMO, but with difference in the amount of feedback required for user selection,

the two schemes yield significantly different sum-rate performance in the practical finite-user case. The SUS-ZFBF method in [5] requires channel state information (CSI) from every user terminal (UT) at the BS, exploits full CSI from all users, and provides a smart selection of users whose channel directions are almost orthogonal ('semi-orthogonal') to yield good performance with ZFBF. On the other hand, the RBF scheme in [4] selects a group of users that are matched to predetermined random orthogonal beam directions, and only requires the feedback of the best beam direction index and the corresponding signal-to-interference-plus-noise ratio (SINR) value from each user. Hence, the feedback overhead is reduced significantly in the RBF scheme. (Note that SUS-ZFBF requires CSI from users, whereas RBF requires channel quality indicator (CQI) from users.) Due to this feedback advantage, the RBF scheme was extended to the correlated channel case [11]. Recently, the RBF scheme was applied to user scheduling in massive MU-MIMO downlink with two-stage beamforming with multiple correlated channel groups [12]. However, it is known that the RBF scheme yields poor performance compared to SUS-ZFBF utilizing full CSI in the practical case of finite users [5].

In this paper, we propose a new user-selection-and-beamforming method for (massive) MU-MIMO downlink that maintains the advantage of SUS-ZFBF, overcomes the disadvantage of RBF, and requires a less amount of feedback than RBF. Our approach starts with identifying the factors that make RBF yield poor sum-rate performance and the factors that make SUS-ZFBF better than RBF in sum-rate performance, and ends with correcting the loss factors associated with RBF and implementing the gain factors associated with SUS-ZFBF without full CSI at the BS. RBF selects a set of users with roughly orthogonal channels. However, as we shall see later in Section III-A, the main loss factors associated with RBF are 1) the criterion of SINR [4] associated with orthogonal beams and 2) the absence of any beam refinement after user selection. *The use of SINR as the selection criterion cannot properly take the channel magnitude into consideration but only considers the angle between each predetermined beam direction and the user channel vector for user selection.* On the other hand, SUS-ZFBF also provides a set of users with semi-orthogonal channel vectors, based on full CSI at the BS. However, SUS-RBF selects semi-orthogonal users with large channel magnitude. Furthermore, SUS-ZFBF performs post-user-selection beam design based on the selected users' CSI, i.e., SUS-ZFBF uses ZFBF for selected users to eliminate the inter-user interference, and the effective channel gain loss associated with ZFBF is managed by controlling the thickness of the user-

selection hyperslab* [5]. Consequently, SUS-ZFBF selects a set of (semi-)orthogonal users with large channel magnitude and the loss associated with ZFBF is made small by increasing the orthogonality of the selected user channel vectors by thinning the user-selection hyperslab when the number of users in the cell increases. As in RBF, we use a set of *orthogonal reference* beam directions, but correct the first loss factor of RBF by defining a new criterion names as *quasi-SINR* that can incorporate the channel magnitude. The user selection is done based on quasi-SINR feedback. Then, we apply post-user-selection ZFBF for selected users. Here, we do control the semi-orthogonality of selected users and the effective channel gain loss associated with ZFBF by defining a user-selection *double cone* around each reference beam direction and by controlling the angle of the user-selection double cone. Under the proposed user selection method, user selection is done based on quasi-SINR, which is a CQI, and the post-user-selection beam refinement is done based on the feedback of CSI from the selected users only. In this way, the main advantage of SUS-ZFBF is implemented in the proposed scheme without full CSI at the BS. The proposed scheduling-and-beamforming method is asymptotically optimal and the proposed method almost achieves the performance of SUS-ZFBF, with significantly reduced feedback overhead which is even less than that required by RBF.

Notation and Organization: We will make use of standard notational conventions. Vectors and matrices are written in boldface with matrices in capitals. All vectors are column vectors. For a matrix \mathbf{A} , \mathbf{A}^T , \mathbf{A}^H , $\text{tr}(\mathbf{A})$, and $[\mathbf{A}]_{i,j}$ indicate the transpose, conjugate transpose, trace, and entry at the i -th row and j -th column of \mathbf{A} , respectively. $\mathbf{A}(:, c_1 : c_2)$ is the submatrix of \mathbf{A} consisting of the columns from c_1 to c_2 . $\text{diag}(\mathbf{A}_1, \dots, \mathbf{A}_n)$ denotes a diagonal matrix composed of diagonal elements $\mathbf{A}_1, \dots, \mathbf{A}_n$. For vector \mathbf{a} , $\|\mathbf{a}\|$ represents the 2-norm of \mathbf{a} . \mathbf{I}_K is the $K \times K$ identity matrix. $\mathbf{x} \sim \mathcal{CN}(\boldsymbol{\mu}, \boldsymbol{\Sigma})$ means that random vector \mathbf{x} is complex Gaussian distributed with mean $\boldsymbol{\mu}$ and covariance matrix $\boldsymbol{\Sigma}$, and $\theta \sim \text{Unif}(a, b)$ means that θ is uniformly distributed for $\theta \in [a, b]$. $\mathbb{E}[\cdot]$ denotes statistical expectation. \mathbb{R} , \mathbb{R}^+ , and \mathbb{C} are the sets of real, non-negative real, and complex numbers, respectively. $\iota = \sqrt{-1}$.

The remainder of this paper is organized as follows. The system model and preliminaries are described in Section II. The proposed user-scheduling-and-beamforming method is presented in Section III and its asymptotic optimality is proved in Section IV. Fairness issues are discussed

*A hyperslab in \mathbb{C}^M is defined as a set $\{\mathbf{w} \in \mathbb{C}^n : \frac{|\mathbf{n}^H \mathbf{w}|}{\|\mathbf{n}\| \|\mathbf{w}\|} \leq \gamma\}$ for a given vector \mathbf{n} and a constant $\gamma > 0$.

in Section V. Numerical results are provided in Section VI, followed by conclusions in Section VII.

II. SYSTEM MODEL AND PRELIMINARIES

We consider massive MU-MIMO downlink. One of the major challenges to implement massive MIMO systems in the real world is the design of a practical precoding architecture for multi-user massive MIMO downlink together with the estimation of channels with high dimensions. Designing precoding vectors or matrices with very high dimensions with the scale of hundred to support a large number of simultaneous UTs without introducing an efficient structure requires heavy computational burden and a huge amount of CSI feedback. One practical precoding solution to multi-user massive MIMO downlink is two-stage beamforming, which is based on a ‘divide-and-conquer’ approach. Recently, Adhikary *et al.* proposed an efficient two-stage beamforming architecture named ‘Joint Spatial Division and Multiplexing (JSDM)’ for multi-user massive MIMO downlink [10]. The key ideas of JSDM are 1) to partition users in a sector (or cell) into multiple groups so that each group has a distinguishable linear subspace spanned by the dominant eigenvectors of the group’s channel covariance matrix and 2) to divide transmit beamforming into two stages based on this grouping, as shown in Fig. 1: The first stage is pre-beamforming that separates multiple groups by using a pre-beamforming matrix designed for each group to filter the dominant eigenvectors of each group’s channel covariance matrix, and the second stage is conventional MU-MIMO precoding that separates and thus simultaneously supports the users within a group based on the effective channel which is given by the product of the pre-beamforming matrix and the actual channel matrix between the antenna array and UTs. One key advantage of such two-stage beamforming is that the pre-beamforming matrices can be designed not based on CSI but based on the channel statistics information, i.e., the channel covariance matrix. The channel statistics information varies slowly compared to CSI and thus can be estimated more easily than CSI, based on some subspace tracking algorithm without knowing instantaneous CSI [13]–[16]. Practically, the channel covariance matrix of a UT can be determined *a priori* based on some side information [10], [17]. Furthermore, the channel covariance matrix associated with a UT or a group in a realistic environment has a much smaller rank than the actual size of the antenna array and therefore, the dimension of the effective channel whose state information is necessary at the BS is significantly reduced since the

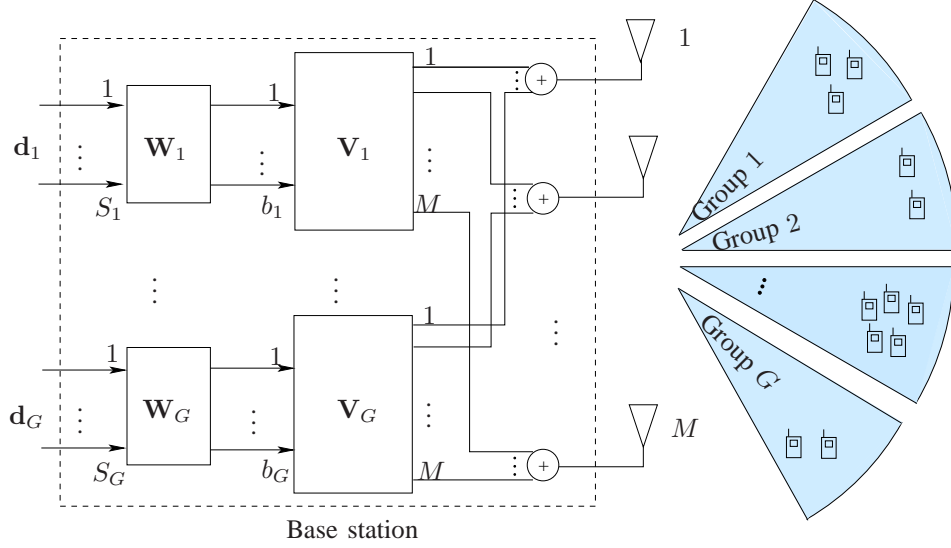


Fig. 1. Multi-group MU-MIMO downlink with two-stage beamforming

effective channel is formed as a precoding matrix and the actual channel matrix with two-stage beamforming.

With the above-mentioned advantages in mind, specifically we consider a single-cell massive MIMO downlink system adopting JSDM composed of a single BS employing M transmit antennas and K single-antenna UTs, as shown in Fig. 1. We consider the large network regime, i.e., $K \gg M$, and assume that the BS chooses S ($\leq M$) users among the K users within the cell and broadcasts independent data streams to the selected users. We assume that the users in the cell are partitioned into G groups such that (s.t.) $\sum_{g=1}^G K_g = K$ and $\sum_{g=1}^G S_g = S$, where K_g and S_g are the number of users and the number of independent data streams in group g , respectively. We also assume that each group has a different channel covariance matrix and every user in a group has the same channel covariance matrix, as in [10]. Then, the $M \times 1$ channel vector \mathbf{h}_{gk} of user k in group g is given by

$$\mathbf{h}_{gk} = \mathbf{U}_g \mathbf{\Lambda}_g^{1/2} \boldsymbol{\eta}_{gk}, \quad (1)$$

where $\mathbf{R}_g = \mathbf{U}_g \mathbf{\Lambda}_g \mathbf{U}_g^H$ is the eigendecomposition of the channel covariance matrix \mathbf{R}_g of group g ; \mathbf{U}_g is the $M \times r_g$ matrix composed of the orthonormal eigenvectors corresponding to the r_g non-zero eigenvalues of \mathbf{R}_g ; $\mathbf{\Lambda}_g$ is the $r_g \times r_g$ diagonal matrix composed of the non-zero

eigenvalues of \mathbf{R}_g ; and $\boldsymbol{\eta}_{g_k} \sim \mathcal{CN}(\mathbf{0}, \mathbf{I}_{r_g})$. Let the elements of \mathbf{U}_g , $\boldsymbol{\Lambda}_g$ and $\boldsymbol{\eta}_{g_k}$ be

$$\mathbf{U}_g = [\mathbf{u}_{g,1}, \mathbf{u}_{g,2}, \dots, \mathbf{u}_{g,r_g}] \quad (2)$$

$$\boldsymbol{\Lambda}_g = \text{diag}(\lambda_{g,1}, \dots, \lambda_{g,r_g}), \quad \lambda_{g,1} > \lambda_{g,2} > \dots > \lambda_{g,r_g} \quad (3)$$

$$\boldsymbol{\eta}_{g_k} = [\eta_{g_k,1}, \eta_{g_k,2}, \dots, \eta_{g_k,r_g}]^T \sim \mathcal{CN}(\mathbf{0}, \mathbf{I}_{r_g}). \quad (4)$$

One widely-used practical channel model is the *one-ring* model introduced by Jakes [18], which captures the situation in which the BS antenna is positioned in high elevation and UTs are surrounded by radio scatters as in a typical urban cell. In the one-ring model, the channel covariance matrix is determined by the angle spread (AS), angle of arrival (AoA), and antenna geometry [19], and in the case of a ULA at the BS with the antenna spacing $\lambda_c D$, the channel covariance matrix is expressed as [19]

$$[\mathbf{R}_t]_{i,j} = \frac{1}{2\Delta} \int_{\theta-\Delta}^{\theta+\Delta} e^{-j2\pi(i-j)D \sin \omega} d\omega, \quad (5)$$

where λ_c is the carrier wavelength, θ is the AoA, and Δ is the AS. One useful thing to note is that with a large uniform linear or planar antenna array (ULA) at the BS, the eigenvectors of the channel covariance matrix reduce to certain columns of the discrete fourier transform (DFT) matrix depending on the AoA and AS of UTs [10], [17].

Denoting the $K_g \times M$ channel matrix for the users in group g by $\mathbf{H}_g = [\mathbf{h}_{g,1}, \dots, \mathbf{h}_{g,K_g}]^H$ and stacking $\{\mathbf{H}_g, g = 1, \dots, G\}$, we have the overall $K \times M$ channel matrix $\mathbf{H} = [\mathbf{H}_1^H, \dots, \mathbf{H}_G^H]^H$. Then, the received signal vector containing all user signals in the cell is given by

$$\mathbf{y} = \mathbf{H}\mathbf{x} + \mathbf{n}, \quad (6)$$

where \mathbf{x} is the $M \times 1$ transmitted signal vector at the BS, $\mathbf{n} \sim \mathcal{CN}(\mathbf{0}, \mathbf{I}_K)$ is the noise vector, and the BS has an average power constraint $\mathbb{E}[\|\mathbf{x}\|^2] \leq P$. In the considered two-stage beamforming, precoding of the data vector \mathbf{d} is done in two steps: first, by a $b \times S$ MU-MIMO precoder \mathbf{W} and then by a $M \times b$ pre-beamformer \mathbf{V} , i.e.,

$$\mathbf{x} = \mathbf{V}\mathbf{W}\mathbf{d},$$

where $\mathbf{d} \sim \mathcal{CN}(\mathbf{0}, \mathbf{I}_S)$. As mentioned earlier, the pre-beamforming matrix $\mathbf{V} = [\mathbf{V}_1, \dots, \mathbf{V}_G]$ is designed based not on the instantaneous CSI but on the channel *statistics* information $\{\mathbf{U}_g, \boldsymbol{\Lambda}_g\}$,

where the $M \times b_g$ submatrix \mathbf{V}_g is the pre-beamforming matrix for group g . Then, the received signal in (6) can be rewritten as [10]

$$\mathbf{y} = \mathbf{G}\mathbf{W}\mathbf{d} + \mathbf{n}, \quad (7)$$

where

$$\mathbf{G} := \mathbf{H}\mathbf{V} = \begin{bmatrix} \mathbf{H}_1\mathbf{V}_1 & \mathbf{H}_1\mathbf{V}_2 & \cdots & \mathbf{H}_1\mathbf{V}_G \\ \mathbf{H}_2\mathbf{V}_1 & \mathbf{H}_2\mathbf{V}_2 & \cdots & \mathbf{H}_2\mathbf{V}_G \\ \vdots & \vdots & \ddots & \vdots \\ \mathbf{H}_G\mathbf{V}_1 & \mathbf{H}_G\mathbf{V}_2 & \cdots & \mathbf{H}_G\mathbf{V}_G \end{bmatrix}. \quad (8)$$

Although the MU-MIMO precoder \mathbf{W} can be designed with full freedom, for simplicity, \mathbf{W} is designed in a block-diagonal form as $\mathbf{W} = \text{diag}(\mathbf{W}_1, \dots, \mathbf{W}_G)$, where \mathbf{W}_g is the $b_g \times S_g$ MU-MIMO precoder and depends on the *effective channel* $\mathbf{G}_g := \mathbf{H}_g\mathbf{V}_g$ for group g only. Hence, in JSDM, the received signal vector for the users in group g is given by

$$\mathbf{y}_g = \mathbf{G}_g\mathbf{W}_g\mathbf{d}_g + \sum_{g' \neq g} \mathbf{H}_g\mathbf{V}_{g'}\mathbf{W}_{g'}\mathbf{d}_{g'} + \mathbf{n}_g, \quad (9)$$

where \mathbf{d}_g and \mathbf{n}_g are the data and noise vectors for group g , respectively. Decomposing \mathbf{G}_g and \mathbf{W}_g as $\mathbf{G}_g = [\mathbf{g}_{g_1}, \dots, \mathbf{g}_{g_{K_g}}]^H$ and $\mathbf{W}_g = [\mathbf{w}_{g_1}, \dots, \mathbf{w}_{g_{K_g}}]$, respectively, we have the received signal of user k in group g (from here on, we will simply say user g_k for user k in group g), given by

$$y_{g_k} = \mathbf{g}_{g_k}^H \mathbf{w}_{g_k} d_{g_k} + \sum_{k' \neq k} \mathbf{g}_{g_k}^H \mathbf{w}_{g_{k'}} d_{g_{k'}} + \sum_{g' \neq g} \mathbf{h}_{g_k}^H \mathbf{V}_{g'} \mathbf{W}_{g'} \mathbf{d}_{g'} + n_{g_k} \quad (10)$$

where \mathbf{g}_{g_k} , \mathbf{w}_{g_k} , d_{g_k} and n_{g_k} are the $b_g \times 1$ effective channel, $b_g \times 1$ MU-MIMO precoding vector, data and noise symbols of user g_k , respectively. Note that the dimension of the effective channel \mathbf{g}_{g_k} for user g_k is reduced to b_g , and $b_g \ll M$ in typical cellular environments with sufficiently high carrier frequency [10]. The second and third terms in the right-hand side (RHS) of (10) are the intra-group and inter-group interference, respectively. Concerning the inter-group interference, we assume that at least the approximate block diagonalization (BD) condition in the below holds [10]:

Condition 1 (Inter-group interference condition [10]):

- *Exact BD*: Each group has a sufficient signal space to transmit S_g data streams, that does not interfere with the signal spaces of other groups, i.e., [10]

$$\dim(\text{span}(\mathbf{U}_g) \cap \text{span}^\perp(\{\mathbf{U}_{g'} : g' \neq g\})) \geq S_g. \quad (11)$$

- *Approximate BD*: When exact BD is impossible, approximate BD can be attained by selecting a matrix \mathbf{U}_g^* consisting of the r_g^* ($\leq r_g$) dominant eigenvectors of the channel covariance matrix for each group g such that [10]

$$\dim(\text{span}(\mathbf{U}_g^*) \cap \text{span}^\perp(\{\mathbf{U}_{g'}^* : g' \neq g\})) \geq S_g. \quad (12)$$

Note that in the case of approximate BD, r_g^* is a control parameter and the inter-group interference still remains in (10) because of the weakest $r_g - r_g^*$ eigenvectors of the channel covariance matrix not included in \mathbf{U}_g^* . Note that both \mathbf{U}_g and \mathbf{U}_g^* have orthonormal columns since they are column-wise submatrices of a unitary matrix. Hence, the average transmit power for user g_k is given by

$$P_{g_k}^{\text{actual}} = \text{tr}(\mathbf{V}_g \mathbf{w}_{g_k} \mathbf{w}_{g_k}^H \mathbf{V}_g^H) = \|\mathbf{w}_{g_k}\|^2 \quad (13)$$

when we set $\mathbf{V}_g = \mathbf{U}_g^*$ for the pre-beamforming matrix, since the variance of d_{g_k} is set to one.

III. THE PROPOSED USER SCHEDULING METHOD

In this section, we propose a user-scheduling-and-beamforming algorithm for a given pre-beamformer $\mathbf{V} = [\mathbf{V}_1, \dots, \mathbf{V}_G]$, adopting ZFBF for the second-stage MU-MIMO precoder \mathbf{W}_g . For the sake of simplicity, we assume $b_g = S_g = r_g^*$ and $\mathbf{V}_g = \mathbf{U}_g^*$ for all g . We also assume that each receiving user g_k (not the BS) knows its *effective* CSI \mathbf{g}_{g_k} .

A. Background

Before presenting the proposed user-scheduling-and-beamforming method, we briefly examine the two disparate user-scheduling-and-beamforming methods in [4] and [5] devised under the linear beamforming framework. For simplicity, let us just consider one group. First, consider the random (orthogonal) beamforming (RBF) in [4]. In this method, the BS just randomly determines a set of orthonormal beam vectors $\{\phi_1, \phi_2, \dots, \phi_{r_g^*}\}$, and then transmits each beam sequentially in time during the training period. In the setting of JSMD, this beam selection corresponds to [12]

$$\phi_i = \mathbf{u}_{g,i}, \quad i = 1, 2, \dots, r_g^* \quad \text{and} \quad \mathbf{W}_g = \mathbf{I}_{r_g^*}. \quad (14)$$

During the training period, user g_k computes the SINR of each beam direction i as [4]

$$\text{SINR}_{g_k,i} = \frac{|\mathbf{h}_{g_k}^H \phi_i|^2}{1 + \sum_{i' \neq i} |\mathbf{h}_{g_k}^H \phi_{i'}|^2}, \quad i = 1, \dots, r_g^*, \quad (15)$$

assuming that $\sum_{i=1}^{r_g^*} d_{\kappa_i} \phi_i$ will be transmitted during the data transmission period, where κ_i is the selected user index for beam direction i . (The inter-group interference is neglected for simplicity.) Then, each user g_k feeds back its maximum SINR value and the corresponding beam index i [4]. After the feedback period is finished, the BS selects a user for each beam direction i such that the selected user for beam direction i has the maximum SINR for the considered beam direction i . (For simplicity, let us neglect the case that one user can be selected for more than one beam direction.) After the selection is done, the BS transmits $\sum_{i=1}^{r_g^*} d_{\kappa_i} \phi_i$ to serve the selected r_g^* users.

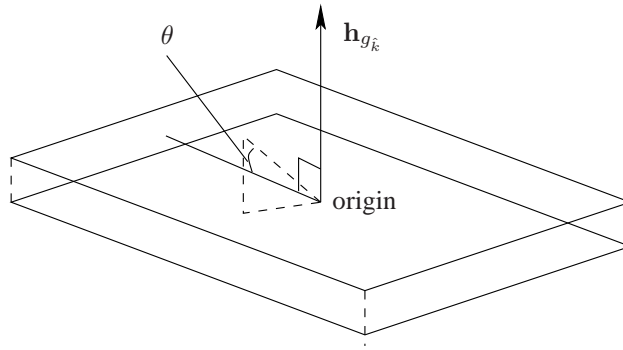


Fig. 2. A hyperslab constructed by an already-included user channel vector

On the other hand, under SUS-ZFBB in [5], the BS collects CSI \mathbf{h}_{g_k} from every UT g_k in the beginning, and sequentially selects r_g^* users by enforcing semi-orthogonality among the selected users. That is, the BS first selects the user that has the largest channel magnitude. Let the firstly selected user's index be $g_{\hat{k}}$. Then, based on the CSI $\mathbf{h}_{g_{\hat{k}}}$, SUS-ZFBB constructs a user-selection hyperslab defined as [5]

$$\mathcal{H}_{g,1} = \left\{ \mathbf{w} \in \mathbb{C}^M : \frac{|\mathbf{h}_{g_{\hat{k}}}^H \mathbf{w}|}{\|\mathbf{h}_{g_{\hat{k}}}\| \cdot \|\mathbf{w}\|} \leq \gamma \right\} \quad (16)$$

as shown in Fig. 2. This means that in Fig. 2, the angle θ is determined to satisfy $\cos \theta \leq \gamma$. Note that if a vector \mathbf{w} is contained in $\mathcal{H}_{g,1}$, \mathbf{w} is semi-orthogonal to $\mathbf{h}_{g_{\hat{k}}}$. Then, SUS-ZFBB selects the user whose channel vector is contained in the hyperslab $\mathcal{H}_{g,1}$ and that has maximum channel vector magnitude within $\mathcal{H}_{g,1}$. After the second user is selected, another hyperslab contained in the first hyperslab is constructed based on the secondly selected user's channel vector. Thus, the newly constructed hyperslab is semi-orthogonal to both the firstly and secondly selected users'

channel vectors. In this way, at each step the user with the largest channel magnitude is selected while semi-orthogonality is maintained among the selected users. Furthermore, the effective channel gain loss associated with later ZFBF can be made small by making the thickness of the hyperslab small for a large number of users in the served cell. (For detail, refer to [5].)

Now, consider RBF explained previously again. First, we examine the SINR defined in (15). Consider a very practical scenario of signal-to-noise ratio (SNR) of 3 dB and four beam directions. Assume that \mathbf{h}_{g_k} has equal size components in $\{\phi_i\}$. Then, $\frac{|\mathbf{h}_{g_k}^H \phi_i|^2}{1} = 2$ and $\sum_{i' \neq i} |\mathbf{h}_{g_k}^H \phi_{i'}|^2 = 6$. (Note that 3GPP LTE-Advanced supports 4×4 or 8×8 MU-MIMO.) Then, it is easy to see that the term '1' in the denominator of the RHS of (15) is negligible, and the SINR becomes

$$\text{SINR}_{g_k, i} \approx \frac{|\mathbf{h}_{g_k}^H \phi_i|^2}{\sum_{i' \neq i} |\mathbf{h}_{g_k}^H \phi_{i'}|^2} = \frac{|\mathbf{h}_{g_k}^H \phi_i|^2 / \|\mathbf{h}_{g_k}\|^2}{\sum_{i' \neq i} |\mathbf{h}_{g_k}^H \phi_{i'}|^2 / \|\mathbf{h}_{g_k}\|^2}. \quad (17)$$

A key point to observe here in (17) is that the SINR is almost *independent of the user channel vector magnitude*! Thus, the user whose channel vector has the *smallest angle* with the given beam direction regardless of its channel magnitude is selected for the given beam direction. (As SNR and the number of streams increase, this effect becomes more evident. Operating SNR of real cellular systems for data (or packet) transmission requiring user scheduling is higher than 3 dB. Note also that when we have only one beam direction, the problem does not occur but in this case, there is no spatial multiplexing.) Of course, this user selection is optimal, when $\mathbf{W}_g = \mathbf{I}$ and thus $\sum_{i=1}^{r_g^*} d_{\kappa_i} \phi_i$ is indeed the transmitted signal. Now, one can see that RBF does not take the channel vector magnitude into account for user selection and furthermore this is because there is no *post-user-selection beam refinement or adjustment*. In RBF, only orthogonality among the selected users is pursued with neglecting the channel magnitude. Compare this with SUS-ZFBF. In SUS-ZFBF, the user with the maximum channel vector magnitude is selected at each inclusion step while semi-orthogonality among the selected users' channels is maintained. In the next subsection, we propose a user-selection-and-beamforming method that corrects the disadvantages of RBF and maintains the advantages of SUS-ZFBF *without* full CSI at the BS.

B. The proposed user selection method

Here, we consider the original two-stage beamforming setting again. (The proposed method can readily be applied to conventional single-stage MU-MIMO downlink too.) As in RBF, we use a set of *orthogonal reference* beam directions, and use $\mathbf{u}_{g,1}, \mathbf{u}_{g,2}, \dots, \mathbf{u}_{g,r_g^*}$ as the orthogonal

reference beam directions here. Then, as in SUS-ZFBF, we enforce semi-orthogonality among the selected users by constructing a *double cone* $\mathcal{C}_{g,i}$ around each reference beam direction i , as shown in Fig. 3, defined as

$$\mathcal{C}_{g,i} = \left\{ \mathbf{h}_{g_k} : \frac{|\mathbf{h}_{g_k}^H \mathbf{u}_{g,i}|}{\|\mathbf{h}_{g_k}\|} \geq \alpha' \right\}, \quad i = 1, 2, \dots, r_g^*, \quad (18)$$

and by checking if the user channel vector \mathbf{h}_{g_k} is contained in $\mathcal{C}_{g,i}$ for each i . (From here on, we will refer to double cone simply as cone.) Note that this checking is done at UTs not at the BS. To construct $\mathcal{C}_{g,i}$, we need the original channel vector \mathbf{h}_{g_k} for user g_k . However, we are assuming that only the equivalent channel state information \mathbf{g}_{g_k} is available at user g_k for the two-stage beamforming. Note that from (8), we have

$$\mathbf{g}_{g_k}^H = \mathbf{h}_{g_k}^H \mathbf{V}_g = \mathbf{h}_{g_k}^H \mathbf{U}_g^* = [\mathbf{h}_{g_k}^H \mathbf{u}_{g,1}, \dots, \mathbf{h}_{g_k}^H \mathbf{u}_{g,r_g^*}]. \quad (19)$$

Hence, the cone-containment checking can be done simply by computing $\frac{\mathbf{g}_{g_k}^H}{\|\mathbf{g}_{g_k}\|}$ and checking if the absolute value of each of its elements is larger than or equal to a new threshold $\alpha \triangleq \alpha' \frac{\|\mathbf{h}_{g_k}\|}{\|\mathbf{g}_{g_k}\|}$, since

$$\frac{\mathbf{g}_{g_k}^H}{\|\mathbf{g}_{g_k}\|} = \frac{\|\mathbf{h}_{g_k}\|}{\|\mathbf{g}_{g_k}\|} \left[\frac{\mathbf{h}_{g_k}^H \mathbf{u}_{g,1}}{\|\mathbf{h}_{g_k}\|}, \dots, \frac{\mathbf{h}_{g_k}^H \mathbf{u}_{g,r_g^*}}{\|\mathbf{h}_{g_k}\|} \right]. \quad (20)$$

Note that $0 \leq \alpha \leq 1$ since each element of the normalized vector $\mathbf{g}_{g_k}^H / \|\mathbf{g}_{g_k}\|$ is compared with α , and α is a system design parameter that controls[†] the semi-orthogonality of the selected user channels. If the channel \mathbf{h}_{g_k} of user g_k is contained in cone i , user g_k 's channel is well aligned with the reference direction i and user g_k belongs to the i -th candidate set. Now, we face the question “which user in the candidate set i should be selected?” Since the semi-orthogonality of users to be selected is already guaranteed by the user-selection cones, we should choose the user in the candidate set i that has the maximum channel vector magnitude. This subsequently answers what should be the CQI that should be feedbacked. In the two-stage beamforming setting with the assumption of the availability of the effective channel \mathbf{g}_{g_k} , we just use $\|\mathbf{g}_{g_k}\|^2$ since

$$\begin{aligned} \|\mathbf{g}_{g_k}\|^2 &= \|\mathbf{h}_{g_k}^H \mathbf{U}_g^*\|^2 = \left\| \left(\sum_{j=1}^{r_g} c_{g_k}^j \mathbf{u}_{g,j} \right)^H \mathbf{U}_g^* \right\|^2 = \sum_{j=1}^{r_g^*} |c_{g_k}^j|^2 \\ &\stackrel{(a)}{\approx} \sum_{j=1}^{r_g} |c_{g_k}^j|^2 = \|\mathbf{h}_{g_k}\|^2, \end{aligned} \quad (21)$$

[†]Controlling α plays the same role as controlling the thickness of the user-selection hyperslab in SUS-ZFBF shown in the previous subsection.

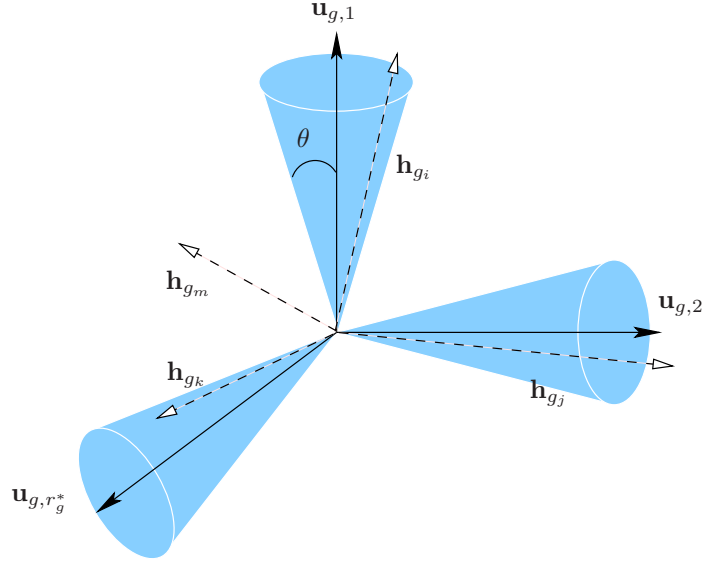


Fig. 3. User selection double cones (the other half of each double cone is not shown)

where $\mathbf{h}_{g_k} = \sum_{j=1}^{r_g^*} c_{g_k,j}^j \mathbf{u}_{g,j}$ with complex linear combination coefficients $c_{g_k,j}$ by (1), and step (a) is valid because the most dominant r_g^* eigenvectors are included. In this way, we can select a set of semi-orthogonal users with large channel magnitude. Once the user selection is done, we do not use $\sum_{i=1}^{r_g^*} d_{\kappa_i} \phi_i$ as the transmit signal as in RBF, but apply ZFBF with water-filling power allocation based on the effective CSI obtained from the selected users. In general, the performance of ZFBF degrades due to noise enhancement in the inversion process and this degradation appears as the effective channel gain loss. However, this effective channel gain loss is managed by the semi-orthogonality of the selected users controlled by the parameter α , as we shall see in Section IV. This post-user-selection beam refinement requires additional effective CSI feedback only from the (a few) selected users.

For further improvement in the two-stage beamforming setting, we can take the inter-group interference into consideration. When $\mathbf{V}_g = \mathbf{U}_g^*$ for all g and equal power $\rho = \frac{P}{\sum_{g=1}^G r_g^*}$ for every scheduled user, the norm of every column of the second-stage beamformer \mathbf{W}_g is ρ from (13). From (10), the average power of the inter-group interference-plus-noise is upper bounded by

$$1 + r_g^* \rho \sum_{g' \neq g} \|\mathbf{h}_{g_k}^H \mathbf{V}_{g'}\|^2 \quad (22)$$

by norm's submultiplicativity and $\|\cdot\| \leq \|\cdot\|_F$, where $\|\cdot\|_F$ is the Frobenius norm. ($\|\mathbf{W}_{g'}\|_F =$

$r_g^*\rho$.) We define a *quasi-SINR* as

$$\mathcal{R}(g_k) := \frac{\|\mathbf{g}_{g_k}\|^2}{\frac{1}{\rho} + r_g^* \sum_{g' \neq g} \|\mathbf{h}_{g_k}^H \mathbf{V}_{g'}\|^2}. \quad (23)$$

In the definition, the intra-group interference does not exist because ZFBF will be used in later post-user-selection beamforming. Without the inter-group interference, the quasi-SINR is simply a scaled version of the square of the effective channel vector magnitude.

Remark 1: The reason for the chosen definition of the quasi-SINR will become clear in Section IV. This metric guarantees the asymptotic optimality of the proposed method under the assumption of the approximated BD in Condition 1 for inter-group interference.

Remark 2: The effective CSI and the average inter-group-interference-plus-noise power can easily be estimated at UTs during the downlink training period. The received signal model (10) at user g_k can be rewritten by combining all intra-group signals as

$$y_{g_k} = \underbrace{\mathbf{h}_{g_k}^H \mathbf{V}_g}_{\mathbf{g}_{g_k}^H} \mathbf{W}_g \mathbf{d}_g + \sum_{g' \neq g} \mathbf{h}_{g_k}^H \mathbf{V}_{g'} \mathbf{W}_{g'} \mathbf{d}_{g'} + n_{g_k}. \quad (24)$$

First, the effective CSI \mathbf{g}_{g_k} can easily be estimated at UTs during the downlink training period. Please see [17] for this. Furthermore, during the downlink training period, the average inter-group interference-plus-noise power $1 + \rho \sum_{g' \neq g} \|\mathbf{h}_{g_k}^H \mathbf{V}_{g'}\|^2$ can also be estimated easily based on (24). That is, the training \mathbf{W}_g and \mathbf{d}_g are known to all UTs in group g . Once \mathbf{g}_{g_k} is estimated at user g_k , user g_k constructs $\mathbf{g}_{g_k}^H \mathbf{W}_g \mathbf{d}_g$, computes $y_{g_k} - \mathbf{g}_{g_k}^H \mathbf{W}_g \mathbf{d}_g = \sum_{g' \neq g} \mathbf{h}_{g_k}^H \mathbf{V}_{g'} \mathbf{W}_{g'} \mathbf{d}_{g'} + n_{g_k}$, squares $y_{g_k} - \mathbf{g}_{g_k}^H \mathbf{W}_g \mathbf{d}_g$, and averages the result over a few training symbol times to obtain the desired value. If the training $\mathbf{W}_{g'}$ and the actual data-transmitting $\mathbf{W}_{g'}$ have similar norm, the estimated average inter-group interference-plus-noise power will be valid for the data-transmission period. Thus, UTs can easily compute the proposed quasi-SINR during the training period.

Now, we present our proposed user-scheduling-and-beamforming algorithm named '*Reference-based Distributed (semi-)Orthogonal user Selection with Post-selection Beam Refinement (ReDOS-PBR)*':

Algorithm 1 (The Proposed User-Scheduling-And-Beamforming Method: ReDOS-PBR):

0) $\alpha \in (0, 1)$ is a pre-determined parameter and is shared by the BS and all UTs. The BS

initializes

$$\mathcal{W}_{g,i} = \emptyset, \text{ for } i = 1, \dots, r_g^* \quad (25)$$

$$\mathcal{S}_g = \emptyset. \quad (26)$$

Every user g_k estimates \mathbf{g}_{g_k} and $1 + \rho \sum_{g' \neq g} \|\mathbf{h}_{g_k}^H \mathbf{V}_{g'}\|^2$.

1) Each user g_k independently computes the following set:

$$\mathcal{I}_{g_k} := \left\{ i : \left| (\mathbf{e}_i^{(g)})^T \frac{\mathbf{g}_{g_k}}{\|\mathbf{g}_{g_k}\|} \right| \geq \alpha, i = 1, \dots, r_g^* \right\}, \quad (27)$$

where $\mathbf{e}_i^{(g)}$ is the i -th column of $\mathbf{I}_{r_g^*}$. $((\mathbf{e}_i^{(g)})^T \frac{\mathbf{g}_{g_k}}{\|\mathbf{g}_{g_k}\|})$ is simply the i -th element of $\frac{\mathbf{g}_{g_k}}{\|\mathbf{g}_{g_k}\|}$.

If user g_k has $\mathcal{I}_{g_k} \neq \emptyset$, then user g_k finds

$$i_{g_k}^* = \arg \max_{i \in \mathcal{I}_{g_k}} \left| (\mathbf{e}_i^{(g)})^T \frac{\mathbf{g}_{g_k}}{\|\mathbf{g}_{g_k}\|} \right| \quad (28)$$

and feedbacks the CQI pair $(i_{g_k}^*, \mathcal{R}(g_k))$ to the BS. If $\mathcal{I}_{g_k} = \emptyset$, user g_k does not feedback.

After the feedback, the BS updates $\mathcal{W}_{g,i_{g_k}^*} \leftarrow \mathcal{W}_{g,i_{g_k}^*} \cup \{k\}$ and stores $\mathcal{R}(g_k)$.

2) For $i = 1, \dots, r_g^*$, the BS finds

$$\kappa_{g,i} = \arg \max_{k \in \mathcal{W}_{g,i}} \mathcal{R}(g_k), \quad (29)$$

and updates

$$\mathcal{S}_g \leftarrow \mathcal{S}_g \cup \{\kappa_{g,i}\}. \quad (30)$$

3) The BS transmits a paging signal to notify that the users in \mathcal{S}_g are scheduled and then, only the corresponding scheduled UTs feedback their effective CSI to the BS. Finally, the BS constructs the MU-MIMO ZFBF precoder with water-filling power allocation for each group based on the signal model (9) and the acquired effective CSI from the scheduled users, and transmits data to the scheduled UTs.

In step 1), each user checks if its channel vector is contained in each of the user-selection cones. If user g_k has a non-empty set \mathcal{I}_{g_k} , then user g_k finds the reference direction that has the largest channel component and feedbacks the corresponding reference direction index $i_{g_k}^*$ and the quasi-SINR $\mathcal{R}(g_k)$ to the BS. If $\mathcal{I}_{g_k} = \emptyset$, then user g_k does not feedback any information to the BS. After the feedback period is over, the BS makes r_g^* candidate sets $\mathcal{W}_{g,1}, \dots, \mathcal{W}_{g,r_g^*}$ for the r_g^* reference directions for group g , based on the CQI feedback information. Here, $\mathcal{W}_{g,i}$ represents the set of users whose channels are contained in the user-selection cone around the

i -th reference direction. In step 2), the BS chooses the user $\kappa_{g,i}$ having the largest quasi-SINR $\mathcal{R}(g_k)$ in each set $\mathcal{W}_{g,i}$, $i = 1, \dots, r_g^*$, to construct the set \mathcal{S}_g of scheduled users for each group g . In step 3), ZFBF is used for the scheduled users. Here, more sophisticated MU-MIMO BF like MMSE BF can also be used for the post-user-selection beam refinement to yield better performance, if additional inter-group interference and noise variance information is available at the BS for the signal model (9). In the case of such advanced post-user-selection beam refinement, $\{\mathbf{W}_g, g = 1, \dots, G\}$ should be designed jointly. However, since the semi-orthogonality among the selected users for each group and the approximated BD condition for inter-group interference are satisfied, ZFBF should be sufficient.

Remark 3 (Amount of feedback): First note that in ReDOS-PBR, user selection is done based on only CQI feedback from possibly all users and post-user-selection beam refinement is done based on the CSI feedback from only the scheduled users. The feedback difference in CQI and CSI is significant in MIMO systems. The amount of feedback required for the proposed method for group g for one scheduling interval is $\sum_{i=1}^{r_g^*} |\mathcal{W}_{g,i}|$ integers for user beam index feedback, $\sum_{i=1}^{r_g^*} |\mathcal{W}_{g,i}|$ real numbers for quasi-SINR feedback, and $2(r_g^*)^2$ real numbers for later effective CSI feedback because only r_g^* users per group need to feedback their effective CSI $\mathbf{g}_{\kappa_{g,i}}$ of complex dimension r_g^* for $\mathbf{V}_g = \mathbf{U}_g^*$. As shown in Lemma 1 in the below, when $\alpha \leq 1/\sqrt{r_g^*}$, \mathcal{I}_{g_k} is a non-empty set for all g_k and thus, every user feedbacks its quasi-SINR to the BS. Hence, in this case, $\sum_{i=1}^{r_g^*} |\mathcal{W}_{g,i}|$ reduces to K_g . When $\alpha > 1/\sqrt{r_g^*}$, on the other hand, $\mathcal{I}_{g_k} = \emptyset$ for some users and thus in this case, $\sum_{i=1}^{r_g^*} |\mathcal{W}_{g,i}|$ can be less than K_g . In Section VI, numerical results show that many users do not feedback even CQI to the BS for optimally chosen α and the feedback overhead is reduced drastically.

Remark 4 (Feedback structure and delay): ReDOS-PBR requires the above-mentioned two-step feedback: The CQI feedback phase and the CSI feedback phase. In practical cellular systems, time is segmented into contiguous radio frames and each radio frame is one scheduling interval. If both feedback phases can be finished within one data transmission radio frame by using some control channel, there is no additional delay in feedback.

Lemma 1: When $\alpha \leq \alpha_{min} := 1/\sqrt{r_g^*}$, \mathcal{I}_{g_k} is a non-empty set for all g_k .

Proof: Suppose that there is a user g_k such that $\mathcal{I}_{g_k} = \emptyset$. Then, $\left| (\mathbf{e}_i^{(g)})^T \frac{\mathbf{g}_{g_k}}{\|\mathbf{g}_{g_k}\|} \right| < 1/\sqrt{r_g^*}$

for all $i = 1, \dots, r_g^*$. Therefore, we have

$$1 = \left\| \frac{\mathbf{g}_{g_k}}{\|\mathbf{g}_{g_k}\|} \right\|^2 = \sum_{i=1}^{r_g^*} \left| (\mathbf{e}_i^{(g)})^T \frac{\mathbf{g}_{g_k}}{\|\mathbf{g}_{g_k}\|} \right|^2 < 1, \quad (31)$$

and have contradiction. Hence, the claim follows. \blacksquare

Remark 5: Lemma 1 implies that $\bigcup_{i=1}^{r_g^*} \mathcal{C}_{g,i} \supset \mathbb{C}^{r_g^*}$ for $\alpha \leq \alpha_{\min} = 1/\sqrt{r_g^*}$. On the other hand, when $\alpha > \frac{1}{\sqrt{2}}$, $\mathcal{C}_{g,i} \cap \mathcal{C}_{g,j} = \emptyset$ for $i \neq j$, because the angle θ in Fig. 3 is $\pi/4$ when $\alpha = 1/\sqrt{2}$.

Lemma 1 and α_{\min} will be useful in Section V.

IV. OPTIMALITY OF THE PROPOSED METHOD

In this section, we prove the asymptotical optimality of the proposed method as $K \rightarrow \infty$. We begin with the optimal sum capacity scaling law of a K -user MIMO broadcast channel consisting of multiple groups with each group's having the same channel covariance matrix, provided in [12].

Theorem 1: [12] In a MU-MIMO downlink system composed of a BS with M transmit antennas and total power constraint P and K users each with a single receive antenna divided into G groups of equal size $K' = K/G = K_g$, where the channel vector of each user in group g is independent and identically distributed (i.i.d.) from $\mathcal{CN}(\mathbf{0}, \mathbf{R}_g)$ for $g = 1, \dots, G$, the sum capacity (which is achieved by DPC) scales as

$$R_{DPC} = \beta \log \log(K') + \beta \log \frac{P}{\beta} + O(1) \quad (32)$$

where $\beta = \min\{M, \sum_{g=1}^G r_g\}$ and $O(1)$ denotes a bounded constant independent of K' , as $K' \rightarrow \infty$.

Proof: See Theorem 1 in [12]. \blacksquare

The same scaling law is achieved by ReDOS-PBR under the approximate BD condition in Condition 1.

Theorem 2: In the system described in Theorem 1, the sum rate of the scheduled sets $\{\mathcal{S}_g\}$ by ReDOS-PBR scales as

$$\mathbb{E} \left[\sum_{g=1}^G R_{ZF,g}(\mathcal{S}_g) \right] \sim R_{DPC}, \quad (33)$$

where $x \sim y$ indicates that $\lim_{K' \rightarrow \infty} x/y = 1$. Here, $R_{ZF,g}(\mathcal{S}_g)$ is the sum rate of the users in \mathcal{S}_g determined by the proposed user-selection method with ZFBF second-stage precoding.

Proof: Similarly to the asymptotic optimality proof of SUS-ZFBF in [5], our proof of the asymptotic optimality of ReDOS-PBR is by showing first that the effective channel gain associated with ReDOS-PBR is bounded below away from zero for some *fixed* α strictly less than one and then showing that the multi-user diversity gain reduction associated with ReDOS-PBR for that fixed α become negligible as $K' \rightarrow \infty$.[‡]

From (9), we have the received signal model for the scheduled users in \mathcal{S}_g as

$$\mathbf{y}_g(\mathcal{S}_g) = \mathbf{G}_g(\mathcal{S}_g) \mathbf{W}_g(\mathcal{S}_g) \mathbf{d}_g(\mathcal{S}_g) + \sum_{g' \neq g} \mathbf{H}_g(\mathcal{S}_g) \mathbf{V}_{g'} \mathbf{W}_{g'} \mathbf{d}_{g'} + \mathbf{n}_g(\mathcal{S}_g), \quad (34)$$

where $\mathbf{W}_g(\mathcal{S}_g) = [\{\mathbf{w}_{g_k}\}_{k \in \mathcal{S}_g}] = [\mathbf{w}_{\kappa_{g,1}}, \dots, \mathbf{w}_{\kappa_{g,r_g^*}}]$ and $\mathbf{G}_g(\mathcal{S}_g) = [\{\mathbf{g}_{g_k}\}_{k \in \mathcal{S}_g}]^H = [\mathbf{g}_{\kappa_{g,1}}, \dots, \mathbf{g}_{\kappa_{g,r_g^*}}]^H$ are respectively the submatrices of \mathbf{W}_g and \mathbf{G}_g corresponding to the users in \mathcal{S}_g obtained by ReDOS-PBR.

i) Lower bound on the effective channel gain: Since ZFBF is assumed for the second-stage beamforming with the signal model (34), we have

$$\begin{aligned} \mathbf{W}_g &:= \mathbf{W}_g(\mathcal{S}_g) = [\mathbf{w}_{\kappa_{g,1}}, \dots, \mathbf{w}_{\kappa_{g,r_g^*}}] \\ &= \mathbf{G}_g^H(\mathcal{S}_g) [\mathbf{G}_g(\mathcal{S}_g) \mathbf{G}_g^H(\mathcal{S}_g)]^{-1} \mathbf{P}_g \\ &=: \tilde{\mathbf{W}}_g \mathbf{P}_g = [\tilde{\mathbf{w}}_{\kappa_{g,1}}, \dots, \tilde{\mathbf{w}}_{\kappa_{g,r_g^*}}] \mathbf{P}_g, \end{aligned} \quad (35)$$

where $\mathbf{P}_g = \text{diag}(\sqrt{P_{\kappa_{g,1}}}, \dots, \sqrt{P_{\kappa_{g,r_g^*}}})$, and $P_{\kappa_{g,i}}$ is the transmit power scaling factor[§] for the scheduled user $\kappa_{g,i} \in \mathcal{S}_g$. Substituting the above ZF $\mathbf{w}_{\kappa_{g,1}}, \dots, \mathbf{w}_{\kappa_{g,r_g^*}}$ into the received signal model (10) of user $\kappa_{g,i}$ yields

$$y_{\kappa_{g,i}} = \sqrt{P_{\kappa_{g,i}}} d_{\kappa_{g,i}} + \sum_{g' \neq g} \mathbf{h}_{g_k}^H \mathbf{V}_{g'} \mathbf{W}_{g'} \mathbf{d}_{g'} + n_{\kappa_{g,i}}, \quad i = 1, \dots, r_g^*, \quad (36)$$

since $\mathbf{G}_g(\mathcal{S}_g) \mathbf{W}_g = \mathbf{P}_g = \text{diag}(\sqrt{P_{\kappa_{g,1}}}, \dots, \sqrt{P_{\kappa_{g,r_g^*}}})$. From (36), the sum rate of the ZF MU-MIMO broadcast channel consisting of users $\{\kappa_{g,1}, \dots, \kappa_{g,r_g^*}\}$ with power scaling $\{P_{\kappa_{g,1}}, \dots, P_{\kappa_{g,r_g^*}}\}$

[‡]We borrowed the flow of our proof from [5]. However, different techniques and ideas are used for our proof of the asymptotic optimality of ReDOS-PBR.

[§]Since the pseudo-inverse $\mathbf{G}_g^H(\mathcal{S}_g) [\mathbf{G}_g(\mathcal{S}_g) \mathbf{G}_g^H(\mathcal{S}_g)]^{-1}$ is fixed for the given set of the scheduled users' effective channel vectors, we need \mathbf{P}_g to control the user power.

is given by [20]

$$R_{ZF,g}(\mathcal{S}_g) = \max_{\{P_{\kappa_{g,i}}\}} \sum_{i=1}^{r_g^*} \log \left(1 + \frac{P_{\kappa_{g,i}}}{1 + \sum_{g' \neq g} \|\mathbf{h}_{g\kappa_{g,i}}^H \mathbf{V}_{g'} \mathbf{W}_{g'}\|^2} \right) \\ \text{s.t.} \quad \sum_{i=1}^{r_g^*} \gamma_{\kappa_{g,i}}^{-1} P_{\kappa_{g,i}} \leq r_g^* \rho, \quad (37)$$

where $r_g^* \rho$ is the total transmit power[¶] assigned to group g ; by (13) the actual power assigned to user $\kappa_{g,i}$ is given by $P_{\kappa_{g,i}}^{\text{actual}} = \|\mathbf{w}_{\kappa_{g,i}}\|^2 = \gamma_{\kappa_{g,i}}^{-1} P_{\kappa_{g,i}}$; and the effective channel gain^{||} $\gamma_{\kappa_{g,i}}$ for user $\kappa_{g,i}$ is given by [5], [21], [22]

$$\gamma_{\kappa_{g,i}} = \frac{1}{[(\mathbf{G}_g(\mathcal{S}_g) \mathbf{G}_g(\mathcal{S}_g)^H)^{-1}]_{i,i}}. \quad (38)$$

This is because $\|\mathbf{w}_{\kappa_{g,i}}\|^2 = \|\tilde{\mathbf{w}}_{\kappa_{g,i}}\|^2 P_{\kappa_{g,i}}$ and $\|\tilde{\mathbf{w}}_{\kappa_{g,i}}\|^2 = [\tilde{\mathbf{W}}_g^H \tilde{\mathbf{W}}_g]_{i,i} = [(\mathbf{G}_g(\mathcal{S}_g) \mathbf{G}_g(\mathcal{S}_g)^H)^{-1}]_{i,i}$.

Now consider the denominator term in the RHS of (38). Since $[\mathbf{G}_g(\mathcal{S}_g) \mathbf{G}_g(\mathcal{S}_g)^H]_{i,j} = \mathbf{g}_{\kappa_{g,i}}^H \mathbf{g}_{\kappa_{g,j}}$, $\forall i, j$, it can be decomposed as

$$\mathbf{G}_g(\mathcal{S}_g) \mathbf{G}_g(\mathcal{S}_g)^H = \mathbf{D} \tilde{\mathbf{G}} \mathbf{D}, \quad (39)$$

where $\mathbf{D} = \text{diag}(\|\mathbf{g}_{\kappa_{g,1}}\|, \dots, \|\mathbf{g}_{\kappa_{g,r_g^*}}\|)$ and

$$\tilde{\mathbf{G}} = \begin{bmatrix} 1 & \tilde{\mathbf{g}}_{\kappa_{g,1}}^H \tilde{\mathbf{g}}_{\kappa_{g,2}} & \cdots & \tilde{\mathbf{g}}_{\kappa_{g,1}}^H \tilde{\mathbf{g}}_{\kappa_{g,r_g^*}} \\ \tilde{\mathbf{g}}_{\kappa_{g,2}}^H \tilde{\mathbf{g}}_{\kappa_{g,1}} & 1 & & \vdots \\ \vdots & & \ddots & \tilde{\mathbf{g}}_{\kappa_{g,r_g^*-1}}^H \tilde{\mathbf{g}}_{\kappa_{g,r_g^*}} \\ \tilde{\mathbf{g}}_{\kappa_{g,r_g^*}}^H \tilde{\mathbf{g}}_{\kappa_{g,1}} & \cdots & \tilde{\mathbf{g}}_{\kappa_{g,r_g^*}}^H \tilde{\mathbf{g}}_{\kappa_{g,r_g^*-1}} & 1 \end{bmatrix} \quad (40)$$

with $\tilde{\mathbf{g}}_{\kappa_{g,i}} = \frac{\mathbf{g}_{\kappa_{g,i}}}{\|\mathbf{g}_{\kappa_{g,i}}\|}$, $\forall i$. Substituting (39) into (38), we have

$$\gamma_{\kappa_{g,i}} = \frac{1}{[(\mathbf{G}_g(\mathcal{S}_g) \mathbf{G}_g(\mathcal{S}_g)^H)^{-1}]_{i,i}} \\ = \frac{1}{[\mathbf{D}^{-1} \tilde{\mathbf{G}}^{-1} \mathbf{D}^{-1}]_{i,i}} \\ = \frac{\|\mathbf{g}_{\kappa_{g,i}}\|^2}{[\tilde{\mathbf{G}}^{-1}]_{i,i}}. \quad (41)$$

[¶] We assume that the total transmit power assigned to group g is proportional to the number of the scheduled users in group g , and hence, it is $r_g^* \rho$.

^{||} Note in the constraint (37) that the ZF loss appears as the shrinkage of the feasible region of $(P_{\kappa_{g,1}}, \dots, P_{\kappa_{g,r_g^*}})$. If $\mathbf{g}_{\kappa_{g,1}}, \dots, \mathbf{g}_{\kappa_{g,r_g^*}}$ are perfectly orthogonal, then $\gamma_{\kappa_{g,i}} = \|\mathbf{g}_{\kappa_{g,i}}\|^2$ and there is no ZF loss.

Consider the term $[\tilde{\mathbf{G}}^{-1}]_{i,i}$ in (41). By Lemma 2 in Appendix A, we have

$$|\tilde{\mathbf{g}}_{\kappa_g,i}^H \tilde{\mathbf{g}}_{\kappa_g,j}| \leq 2\alpha\sqrt{1-\alpha^2} \text{ for } i \neq j \quad (42)$$

when $\alpha \geq 1/\sqrt{2}$. By the Gershgorin circle theorem [23] and (42), every eigenvalue of the Hermitian matrix $\tilde{\mathbf{G}}$ is in a Gershgorin disk,** i.e.,

$$\begin{aligned} \lambda(\tilde{\mathbf{G}}) &\in \{z \in \mathbb{R}^+ : |z - 1| \leq (r_g^* - 1)2\alpha\sqrt{1-\alpha^2}\}, \\ &= \{z \in \mathbb{R}^+ : 1 - (r_g^* - 1)2\alpha\sqrt{1-\alpha^2} \leq z \leq 1 + (r_g^* - 1)2\alpha\sqrt{1-\alpha^2}\} \end{aligned} \quad (43)$$

where $\lambda(\tilde{\mathbf{G}})$ is the set of eigenvalues of $\tilde{\mathbf{G}}$. When $(r_g^* - 1)2\alpha\sqrt{1-\alpha^2} < 1$, equivalently,

$$\alpha > \sqrt{\frac{1 + \sqrt{\frac{r_g^* - 2}{r_g^* - 1}}}{2}}, \quad (44)$$

we have a non-trivial lower bound on $\lambda_{\min}(\tilde{\mathbf{G}})$ and

$$[\tilde{\mathbf{G}}^{-1}]_{i,i} \leq [\lambda_{\min}(\tilde{\mathbf{G}})]^{-1} \stackrel{(a)}{\leq} \frac{1}{1 - (r_g^* - 1)2\alpha\sqrt{1-\alpha^2}}, \quad (45)$$

since $\tilde{\mathbf{G}}$ is self-adjoint and (a) follows from (43), where $\lambda_{\min}(\tilde{\mathbf{G}})$ is the minimum eigenvalue of $\tilde{\mathbf{G}}$. Thus, from (41) and (45), the effective channel gain $\gamma_{\kappa_g,i}$ is lower bounded by

$$\gamma_{\kappa_g,i} \geq \frac{\|\mathbf{g}_{\kappa_g,i}\|^2}{\frac{1}{1 - (r_g^* - 1)2\alpha\sqrt{1-\alpha^2}}}. \quad (46)$$

Note that the derived lower bound (46) on the effective channel gain is valid for any *fixed* α satisfying

$$\alpha > \sqrt{\frac{1 + \sqrt{\frac{r_g^* - 2}{r_g^* - 1}}}{2}} \stackrel{(a)}{\geq} \frac{1}{\sqrt{2}}, \quad (47)$$

where (a) for the validity of (42) is valid for any $r_g^* \geq 2$. By making $\alpha \uparrow 1$, we can completely eliminate the ZFBF loss. However, $\alpha \uparrow 1$ will lose the multiuser diversity gain. So, we fix α to an arbitrary number $\bar{\alpha}$ strictly less than one, independent of K' such that

$$\bar{\alpha} \in \left(\sqrt{\frac{1 + \sqrt{\frac{r_g^* - 2}{r_g^* - 1}}}{2}}, 1 \right). \quad (48)$$

**All Gershgorin disks of $\tilde{\mathbf{G}}$ have the same center of one and the same radius upper bound. So, we can use any of the Gershgorin disks of $\tilde{\mathbf{G}}$.

ii) *Multi-user diversity gain*: There are several difficult points in handling the multi-user diversity gain of ReDOS-PBR with the multi-group setting of JSMD. The first point is that only users whose channel vectors are contained in one of the user-selection cones report quasi-SINR and the second point is that we should handle the inter-group interference properly. Despite such difficulty we were able to show that the multi-user diversity gain is still preserved for ReDOS-PBR under the approximate BD condition. The main insight is that with fixed $\bar{\alpha}$ in (48) strictly less than one, independent of K' , the number of users whose channel vectors are contained in each user-selection cone tends to infinity as $K' \rightarrow \infty$ since each user-selection cone occupies certain fixed non-trivial measure (or volume) in $\mathbb{C}^{r_g^*}$.

As in [5], the first difficulty mentioned above can be handled by defining

$$\phi_{g_k}^i = \begin{cases} \mathcal{R}(g_k), & k \in \mathcal{W}_{g,i}, \\ 0, & \text{otherwise} \end{cases} \quad (49)$$

for all users $k = 1 \dots, K_g = K'$ in group g . Then, for a given i , the random variable $\phi_{g_k}^i$ is i.i.d. across k in the same group g since $\mathbf{h}_{g_k} \stackrel{i.i.d.}{\sim} \mathcal{CN}(\mathbf{0}, \mathbf{R}_g)$. Note that

$$\kappa_{g,i} = \arg \max_{k \in \mathcal{W}_{g,i}} \mathcal{R}(g_k) = \arg \max_{k \in \{1, \dots, K_g = K'\}} \phi_{g_k}^i. \quad (50)$$

The multi-user diversity gain results from choosing the best user among all users with i.i.d. channel realizations. However, with ReDOS-PBR, for each data stream, the best user within $\mathcal{W}_{g,i}$ is chosen, and thus there exists some loss in the multi-user diversity gain. However, based on extreme value theory we have that for each i

$$\Pr\{\phi_{\kappa_{g,i}}^i > u_g^i\} \geq 1 - O(1/K'), \quad (51)$$

for ReDOS-PBR under the approximate BD condition in Condition 1, where

$$u_g^i = (\lambda_{g,1} \log K' - \lambda_{g,1} \log \log K' + a_i) / (1/\rho + \epsilon); \quad (52)$$

$\lambda_{g,1}$ is the maximum eigenvalue of \mathbf{R}_g (see (3)); and a_i and ϵ are constants independent of K' . Proof of (51, 52) is in Appendix C with some prerequisite on extreme value theory in Appendix B.

iii) Finally, we show the asymptotic optimality (33) of ReDOS-PBR based on *i*) and *ii*). Fix α as $\bar{\alpha}$ in (48). Then, we have

$$\begin{aligned}
& \mathbb{E} \left[\sum_{g=1}^G R_{ZF,g}(\mathcal{S}_g) \right] \\
& \stackrel{(a)}{\geq} \mathbb{E} \left[\sum_{g=1}^G \sum_{i=1}^{r_g^*} \log \left(1 + \frac{\rho \gamma_{\kappa_{g,i}}}{1 + \sum_{g' \neq g} \|\mathbf{h}_{\kappa_{g,i}}^H \mathbf{V}_{g'} \mathbf{W}_{g'}\|^2} \right) \right] \\
& \stackrel{(b)}{\geq} \mathbb{E} \left[\sum_{g=1}^G \sum_{i=1}^{r_g^*} \log \left(1 + \frac{\|\mathbf{g}_{\kappa_{g,i}}\|^2 [1 - (r_g^* - 1)2\alpha\sqrt{1 - \alpha^2}]}{\frac{1}{\rho} + r_g^* \sum_{g' \neq g} \|\mathbf{h}_{\kappa_{g,i}}^H \mathbf{V}_{g'}\|^2} \right) \right] \\
& \stackrel{(c)}{\geq} \sum_{g=1}^G \sum_{i=1}^{r_g^*} \Pr\{\phi_{\kappa_{g,i}}^i > u_g^i\} \log \left(1 + u_g^i [1 - (r_g^* - 1)2\alpha\sqrt{1 - \alpha^2}] \right) \\
& \stackrel{(d)}{\geq} \sum_{g=1}^G \sum_{i=1}^{r_g^*} \left[1 - O\left(\frac{1}{K'}\right) \right] \log \left(1 + u_g^i [1 - (r_g^* - 1)2\alpha\sqrt{1 - \alpha^2}] \right) \\
& \stackrel{(e)}{\sim} \sum_{g=1}^G \sum_{i=1}^{r_g^*} \log \left(1 + \left(\frac{1 - (r_g^* - 1)2\alpha\sqrt{1 - \alpha^2}}{1/\rho + \epsilon} \right) \lambda_{g,1} \log K' \right) \tag{53}
\end{aligned}$$

$$\stackrel{(f)}{\sim} \sum_{g=1}^G r_g^* \log(1 + \rho \lambda_{g,1} \log K') \tag{54}$$

$$\sim \left(\sum_{g=1}^G r_g^* \right) \log \rho + \sum_{g=1}^G r_g^* \log \lambda_{g,1} + \left(\sum_{g=1}^G r_g^* \right) \log \log K' \tag{55}$$

where (a) follows from the suboptimal equal power allocation $\rho = \frac{P}{\sum_{g=1}^G r_g^*} = \|\mathbf{w}_{\kappa_{g,i}}\|^2 = \gamma_{\kappa_{g,i}}^{-1} P_{\kappa_{g,i}}, \forall g, i$; (b) is obtained by (46) and (22) valid for $\bar{\alpha}$; (c) holds by the definition (23) of quasi-SINR $\mathcal{R}(g_k)$ and the definition (49) of $\phi_{g_k}^i$, and $\mathbb{E}f(X) = \int_0^\infty f(x)p(x)dx \geq \Pr(X \geq u)f(u)$ for a monotone increasing function f (here, $f = \log$); (d) holds by (51); (e) follows from $(1 - O(1/K')) \sim 1$ and $u_g^i \sim (\lambda_{g,1} \log K')/(1/\rho + \epsilon)$ from (52); and (f) follows since the difference between the two logarithmic terms in (53) and (54) converges to a constant independent of K' , given by

$$\sum_{g=1}^G r_g^* \log \left(\frac{1 + \rho\epsilon}{1 - (r_g^* - 1)2\alpha\sqrt{1 - \alpha^2}} \right).$$

Finally, consider (55). In both cases of $\sum_{g=1}^G r_g < M$ and $\sum_{g=1}^G r_g \geq M$, we can choose r_g^* such that $\sum_{g=1}^G r_g^* = \min\{M, \sum_{g=1}^G r_g\} = \beta$. Then, (55) is the same as (32) since $P/\beta = \rho$. ■

Note that fixed α in the range of (48) *guarantees* the asymptotic optimality of ReDOS-PBR. We do not know whether α outside this range yields asymptotic optimality or not. (This depends on the tightness of the bound given by the Gershgorin circle theorem used in (43).) For proof of asymptotic optimality, the existence of one α value, i.e., $\bar{\alpha}$, is sufficient. In the practical case of *finite* users in the cell, optimal α may be smaller than $\sqrt{1 + \sqrt{\frac{r_g^* - 2}{r_g^* - 1}}}$. Numerical results in Section VI shows that the performance of ReDOS-PBR in the finite-user case is quite insensitive to α .

V. EXTENSION

In the previous section, we only discussed user selection and beamforming for maximizing the sum rate. Now, consider fairness among users. If the channel statistics are the same across users and the channel realizations are i.i.d. across scheduling intervals, the fairness issue will be resolved automatically [9]. However, in slow-fading environments or in practical downlink systems with different large-scale fading for users at different locations, some scheme should be implemented to impose fairness among users. Among several well-known fairness-imposing schemes [5], [9], [24], we here consider the round-robin (RR) scheme and the proportional fairness (PF) scheme, and modify ReDOS-PBR in the previous section for RR and PF. During this modification, we exploit the degree-of-freedom associated with the parameter α of ReDOS-PBR (i.e., cone-containment checking is done at UTs and α can be adapted properly) and the fact that every UT reports CQI when $\alpha \leq \alpha_{min}$ by Lemma 1.

A. ReDOS-PBR for Round Robin

There can be many modified versions ReDOS-PBR for RR (ReDOS-PBR-RR). Here we consider the following modified scheme. In RR, all users should be served in one round of scheduling. For this, we successively apply ReDOS-PBR to each scheduling interval with controlling α , until no unserved users are left. For the proposed ReDOS-PBR-RR, we assume that α is adapted at the BS every scheduling interval and there exists a downlink broadcasting control channel that informs every UT of the new α value each scheduling interval.

Since large α reduces the effective channel gain loss of the assumed ZFBF, large α is desired from the perspective of the effective channel gain. However, when α is too large (close to 1), we would have $\mathcal{W}_{g,i} = \emptyset$ for some i , even though there are some users whose channels are roughly aligned to the i -th reference direction. In this case, no user will be selected for the i -th reference

direction and the spatial multiplexing gain will be reduced. Such an event can be avoided by reducing α . In the proposed ReDOS-PBR-RR, to detect such an event, every UT feeds back the most aligned reference direction index $i_{g_k}^*$ all the time, but feeds back $\mathcal{R}(g_k)$ only when the user's channel vector is contained in the cone $\mathcal{C}_{g,i_{g_k}^*}$. After the BS collects CQI from all UTs, the BS checks if there exists a reference direction index that has no associated $\mathcal{R}(g_k)$ feedback. Then, the BS knows whether the current α value is too high or not.

We now present the proposed ReDOS-PBR-RR trying to attain good trade-off between the effective channel gain and the spatial multiplexing gain by exploiting the considered CQI feedback strategy.

Algorithm 2 (ReDOS-PBR-RR):

- 0) Initialize $\alpha_g(1) \in [\alpha_{min}, 1)$, $\Delta_\alpha > 0$, $\mathcal{K}_g = \{1, \dots, K_g\}$, and $t = 1$.
- 1) At the scheduling interval t , choose the set $\mathcal{S}_g(t)$ of users among the users in \mathcal{K}_g by ReDOS-PBR with $\alpha_g(t)$. On the contrary to the original ReDOS-PBR, every user with $\mathcal{I}_{g_k} = \emptyset$ also feeds back its reference direction index without the corresponding quasi-SINR in the CQI feedback phase for the modified version.
- 2) If $|\mathcal{S}_g(t)| < r_g^*$, update $\alpha_g(t+1) \leftarrow \alpha_g(t) - \Delta_\alpha$. (That is, target more spatial multiplexing gain.) If $|\mathcal{S}_g(t)| = r_g^*$, update $\alpha_g(t+1) \leftarrow \alpha_g(t) + \Delta_\alpha$. (That is, target more effective channel gain.) When $\alpha_g(t+1) \notin [\alpha_{min}, 1)$, $\alpha_g(t+1) \leftarrow \alpha_g(t)$. The new $\alpha(t+1)$ is broadcast to all UTs.
- 3) Page the selected users $\mathcal{S}_g(t)$, obtain CSI from them, transmit data to them with ZFBF, and update $\mathcal{K}_g \leftarrow \mathcal{K}_g \setminus \mathcal{S}_g(t)$.
- 4) If $\mathcal{K}_g \neq \emptyset$, update $t \leftarrow t + 1$ and go to step 1). Otherwise, stop.

B. ReDOS-PBR for Proportional Fairness

The proportionally fair (PF) scheduling algorithm exploits multiuser diversity gain with consideration of fairness [9]. In the single-input single-output (SISO) PF algorithm, the BS keeps track of the average past served rate μ_{g_k} for each user g_k and selects the user that has the maximum of the current supportable rate $R_{g_k}(t) = \log(1 + |h_{g_k}(t)|^2)$ (determined by the user's current channel state) divided by the user's past average served rate μ_{g_k} . That is, the selection criterion is $\frac{R_{g_k}(t)}{\mu_{g_k}}$ and the average served rate is updated by a simple first-order autoregressive

(AR) filter as

$$\mu_{g_k}(t+1) = (1-\delta)\mu_{g_k}(t) + \delta R_{g_k}(t)I_{\{g_k \in \mathcal{S}_g(t)\}}, \quad (56)$$

where I_A is the indicator function of event A , and $\mathcal{S}_g(t)$ is the set of scheduled users at time t . In [5], the PF algorithm was extended to incorporate MIMO situation and was applied to SUS-ZFBF. The main difference between the SISO and MIMO cases is that the supportable rate $R(g_k, \mathcal{S}_g(t))$ of each user g_k cannot be computed before user selection, because the rate itself depends on the user selection in the MIMO case. However, this difficulty was intelligently circumvented in [5], based on the semi-orthogonality of the selected users. Since ReDOS-PBR also possesses the semi-orthogonality among the selected users, we can apply the same idea as that in [5] here. Since the selected users are semi-orthogonal, we approximate the supportable rate simply by

$$R(g_k, \mathcal{S}_g(t)) \approx \log(1 + \mathcal{R}(g_k)) =: \hat{R}(g_k)(t). \quad (57)$$

Thus, in the modified ReDOS-PBR for proportional fairness (ReDOS-PBR-PF), for each reference direction, after the CQI feedback phase, we select

$$\kappa_{g,i} = \arg \max_{k \in \mathcal{W}_{g,i}} \frac{\hat{R}(g_k)(t)}{\mu_{g_k}(t)} \quad \text{for } i = 1, \dots, r_g^*. \quad (58)$$

Then, the BS collects CSI from the selected users, transmits data after post-selection beam refinement, computes the exact served rate for the scheduled users, and update μ_{g_k} by (56).

One requirement for ReDOS-PBR-PF to compute (58) for all users at each scheduling interval t is that all users should report their CQI (the reference beam index and quasi-SINR) to the BS at every interval t . This can be done simply by setting $\alpha = \alpha_{min}$ for all users by Lemma 1. However, CQI feedback can be reduced by exploiting the property of PF itself and distributed and individual control α at each UT. Note that once a user g_k is served, μ_{g_k} increases suddenly and the selection criterion in (58) decreases suddenly. Hence, user g_k will not be selected in the next scheduling interval unless user g_k 's channel vector at the next scheduling interval is highly aligned with some reference beam direction with large magnitude. Therefore, the served user can increase its own α denoted by $\alpha_{g_k}(t)$ suddenly by some step $\Delta_{\alpha,up}$, targeting bigger chance for good channel realization. When the user is not served, α_{g_k} is reduced by $\Delta_{\alpha,down}$ (say, $\Delta_{\alpha,down} = \Delta_{\alpha,up}/T$ with $T > 1$). Then, $\alpha_{g_k}(t)$ comes back to α_{min} in some time and user g_k surely reports CQI again. Here, $\Delta_{\alpha,up}$ and $\Delta_{\alpha,down}$ are system design parameters which

should be determined properly. Note that $\Delta_{\alpha,up}$ and $\Delta_{\alpha,down}$ can be used not only for feedback reduction but also for fairness enhancement, since it is highly likely that a served user will not be served again successively. Such an efficient semi-orthogonality and feedback control is possible for ReDOS-PBR because cone-containment checking for semi-orthogonality is done individually at UTs. Summarizing the above-mentioned idea, we now present the proposed ReDOS-PBR-PF:

Algorithm 3 (ReDOS-PBR-PF):

- 0) Initialize $\alpha_{g_k}(1) = \alpha_{min}$, $\mu_{g_k}(1) = \mu > 0$, $\forall g, k$, and $t = 1$, and $\Delta_{\alpha,up} > \Delta_{\alpha,down} > 0$. (Now each user has its own $\alpha_{g_k}(t)$.)
- 1) At time t , each user g_k computes \mathcal{I}_{g_k} in (27) based on its own $\alpha_{g_k}(t)$. Then, follow the remaining sub-steps in step 1) of original ReDOS-PBR.
- 2) The BS chooses the set of users $\mathcal{S}_g(t)$ by computing (58) after the CQI feedback phase.
- 3) After the CSI feedback phase, the BS serves the scheduled users in $\mathcal{S}_g(t)$ with ZFBF. Then, the BS updates $\mu_{g_k}(t)$ according to (56) with the actually served rate $R(g_k, \mathcal{S}_g(t))$.
- 4) The users in $\mathcal{S}_g(t)$ update $\alpha_{g_k}(t+1) \leftarrow \alpha_{g_k}(t) + \Delta_{\alpha,up}$ and other unserved users update $\alpha_{g_k}(t+1) \leftarrow \alpha_{g_k}(t) - \Delta_{\alpha,down}$. (Users know whether they are served or not during the scheduled user paging time.) When $\alpha_{g_k}(t+1) \notin [\alpha_{min}, 1)$, $\alpha_{g_k}(t+1) \leftarrow \alpha_{g_k}(t)$.
- 5) Update $t \leftarrow t + 1$ and go to step 1).

In the above algorithm, UTs exploit α for efficient CQI feedback control, but UTs can exploit $\hat{R}(g_k)(t)$ in addition to $\alpha_{g_k}(t)$ for the same purpose since each UT can compute $\hat{R}(g_k)(t) = \log(1 + \mathcal{R}(g_k))$ by itself. There can be various ways to combine $(\alpha_{g_k}(t), \hat{R}_{g_k}(t))$ for efficient distributed CQI feedback control.

Remark 6 (On extension to the case of UTs with multiple receive antennas): ReDOS-PBR can be extended without difficulty to the case in which UTs have multiple receive antennas. In this case, each antenna can be regarded as a different user, and ReDOS-PBR for single-antenna UTs can be applied [5]. Here, a UT with multiple receive antenna imposes a restriction that the candidate set for one receive antenna and that of another receive antenna are different.

VI. NUMERICAL RESULTS

In this section, we provide some numerical results regarding the proposed user-scheduling-and-beamforming method. First, we verified the asymptotic analysis in Section IV. To verify the

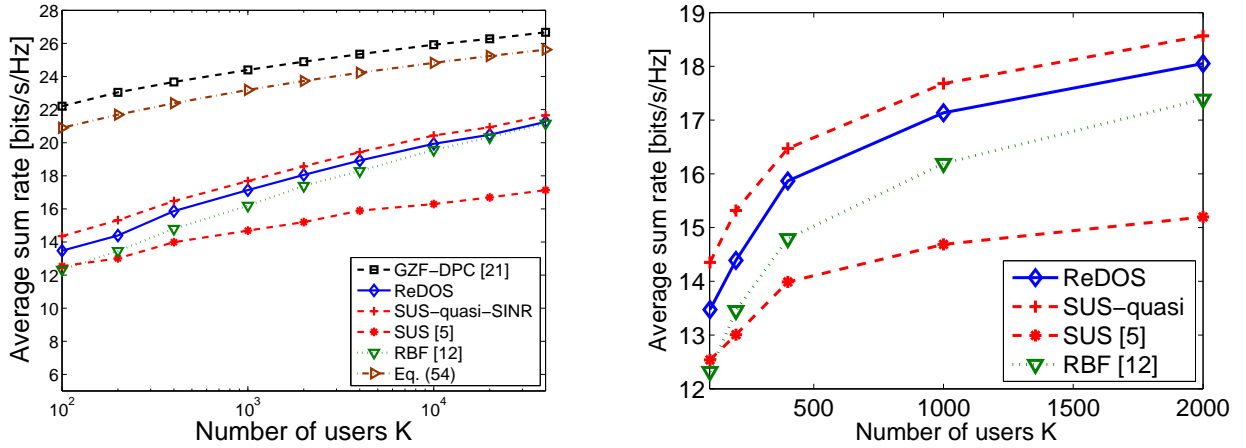


Fig. 4. Multi-group performance: (a) average sum rate w.r.t. the number of users and (b) the same figure as (a) with the range from $K = 100$ to $K = 2000$

asymptotic analysis, we considered a small MISO downlink system (with two groups ($G = 2$) and inter-group interference) to which DPC-based beamforming [21] can be applied. The system consisted of a BS with four transmit antennas ($M = 4$) and $P = 15$ dB and K single-antenna UTs, and the channel vectors were independently generated according to the model (1) with $\mathbf{R}_1 = \mathbf{U}_1 \mathbf{\Lambda}_1 \mathbf{U}_1^H$ and $\mathbf{R}_2 = \mathbf{U}_2 \mathbf{\Lambda}_2 \mathbf{U}_2^H$, where $\mathbf{U}_1 = \mathbf{F}_{DFT}^{(4)}(:, 1 : 3)$, $\mathbf{U}_2 = \mathbf{F}_{DFT}^{(4)}(:, 3 : 4)$, $\mathbf{\Lambda}_1 = \text{diag}(1, r, r^2)$, $\mathbf{\Lambda}_2 = \text{diag}(1, r)$, $r = 0.7$, and $\mathbf{F}_{DFT}^{(4)}$ is the 4-point discrete Fourier transform (DFT) matrix. The pre-beamformer matrices were chosen as $\mathbf{V}_1 = \mathbf{U}_1^* = \mathbf{U}_1(:, 1 : 2)$ and $\mathbf{V}_2 = \mathbf{U}_2^* = \mathbf{U}_2$ to satisfy the approximate BD condition in Condition 1. Fig. 4 shows the result. In the figure, the performance of the DPC-based beamforming in [21] is shown as the performance reference. (In [21], the authors proposed a greedy user selection method based on QR decomposition and the assumption of the availability of DPC.) It is seen that the predicted asymptotic scaling behavior of ReDOS-PBR shown in eq. (54) has the same slope as the DPC-based user selection method in [21]. The actual finite-user sum-rate behavior of several algorithms is also shown in Fig. 4. We considered ReDOS-PBR, RBF in [12], the original SUS-ZFBB in [5], and a modified SUS-ZFBB using quasi-SINR in (23). (Since the original SUS-ZFBB with the channel norm criterion was proposed for the single-cell (or single-group) case, we considered SUS-ZFBB with quasi-SINR for the multi-group case for fair comparison.) It is seen that SUS-ZFBB with quasi-SINR, ReDOS-PBR and RBF all follow the slope of the DPC-based scheme

as expected. It is also seen that SUS-ZFBF with the norm criterion does not handle inter-group interference properly. As expected, SUS-ZFBF (with quasi-SINR) performs best, RBF performs worst, and ReDOS-PBR is in-between. In the considered small system case, the performance difference between the three algorithms is not so significant.

With the asymptotic scaling behavior w.r.t. K verified, we considered a more realistic scenario. We considered a MISO downlink system where a BS with $P = 15$ dB was equipped with a ULA of $M = 32$ antenna elements and each of K UTs had a single receive antenna. The UTs were grouped into eight groups ($G = 8$), and the BS served four UTs ($r_g^* = 4$) simultaneously for each group. The channel covariance matrix and the pre-beamformer matrix of each group were chosen as

$$\begin{aligned} \mathbf{U}_1 &= \mathbf{F}_{DFT}^{(32)}[:, 1 : 5], \quad \mathbf{V}_1 = \mathbf{U}_1^* = \mathbf{U}_1[:, 1 : 4] (= \mathbf{F}_{DFT}^{(32)}[:, 1 : 4]) \\ \mathbf{U}_2 &= \mathbf{F}_{DFT}^{(32)}[:, 5 : 9], \quad \mathbf{V}_2 = \mathbf{U}_2^* = \mathbf{U}_2[:, 1 : 4] (= \mathbf{F}_{DFT}^{(32)}[:, 5 : 8]) \\ \mathbf{U}_3 &= \mathbf{F}_{DFT}^{(32)}[:, 9 : 13], \quad \mathbf{V}_3 = \mathbf{U}_3^* = \mathbf{U}_3[:, 1 : 4] (= \mathbf{F}_{DFT}^{(32)}[:, 9 : 12]) \\ \mathbf{U}_4 &= \mathbf{F}_{DFT}^{(32)}[:, 13 : 17], \quad \mathbf{V}_4 = \mathbf{U}_4^* = \mathbf{U}_4[:, 1 : 4] (= \mathbf{F}_{DFT}^{(32)}[:, 13 : 16]) \\ \mathbf{U}_5 &= \mathbf{F}_{DFT}^{(32)}[:, 17 : 21], \quad \mathbf{V}_5 = \mathbf{U}_5^* = \mathbf{U}_5[:, 1 : 4] (= \mathbf{F}_{DFT}^{(32)}[:, 17 : 20]) \\ \mathbf{U}_6 &= \mathbf{F}_{DFT}^{(32)}[:, 21 : 25], \quad \mathbf{V}_6 = \mathbf{U}_6^* = \mathbf{U}_6[:, 1 : 4] (= \mathbf{F}_{DFT}^{(32)}[:, 21 : 24]) \\ \mathbf{U}_7 &= \mathbf{F}_{DFT}^{(32)}[:, 25 : 29], \quad \mathbf{V}_7 = \mathbf{U}_7^* = \mathbf{U}_7[:, 1 : 4] (= \mathbf{F}_{DFT}^{(32)}[:, 25 : 28]) \\ \mathbf{U}_8 &= \mathbf{F}_{DFT}^{(32)}[:, 29 : 32], \quad \mathbf{V}_8 = \mathbf{U}_8^* = \mathbf{U}_8 (= \mathbf{F}_{DFT}^{(32)}[:, 29 : 32]), \end{aligned}$$

where $\mathbf{F}_{DFT}^{(32)}$ is the 32-point DFT matrix, and $\mathbf{\Lambda}_i = \text{diag}(1, r, r^2, r^3, r^4)$ with $r = 0.6$ for $i = 1, \dots, 7$ and $\mathbf{\Lambda}_8 = \text{diag}(1, r, r^2, r^3)$. This setting of channel covariance matrices and pre-beamformer matrices satisfies the approximate BD condition. Fig. 5 (a) shows the sum-rate performance of the three schemes: SUS-ZFBF, RBF, and ReDOS-PBR. 200 independent channel realizations according to (1) were used for each K and the average sum rate is the average over the 200 channel realizations. (For the figure, the user-selection hyperslab thickness for SUS-ZFBF and the user-selection cone angle for ReDOS-PBR were optimally chosen for each K .)

Now it is seen that the performance gap between SUS-ZFBF with quasi-SINR and RBF is significant. It is also seen that proposed ReDOS-PBR closely follows SUS-ZFBF with quasi-SINR. Fig. 5 (b) shows the amount of feedback for the same setting as in 5 (a). As expected,

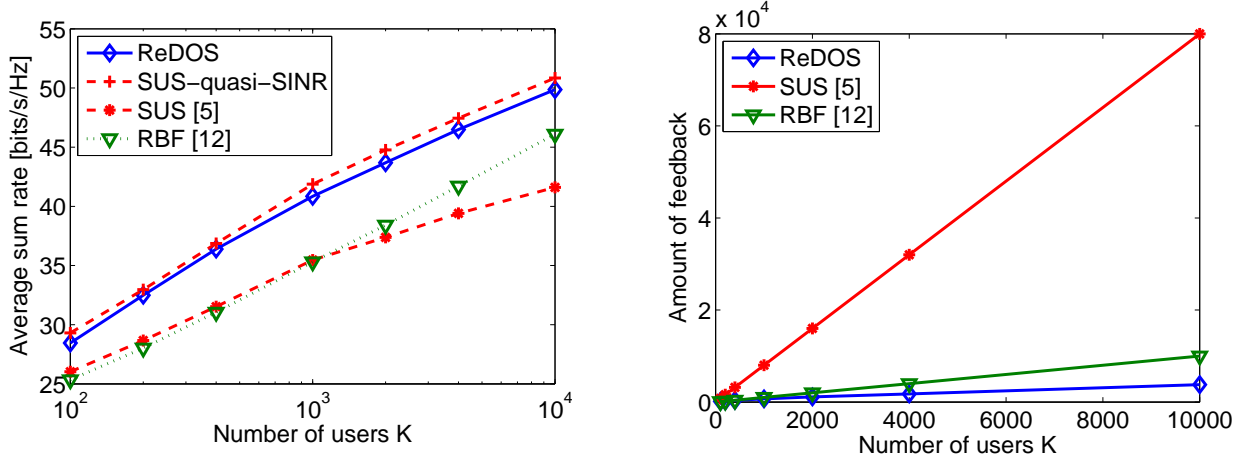


Fig. 5. Multi-group performance: (a) average sum rate performance and (b) amount of feedback (number of required real numbers)

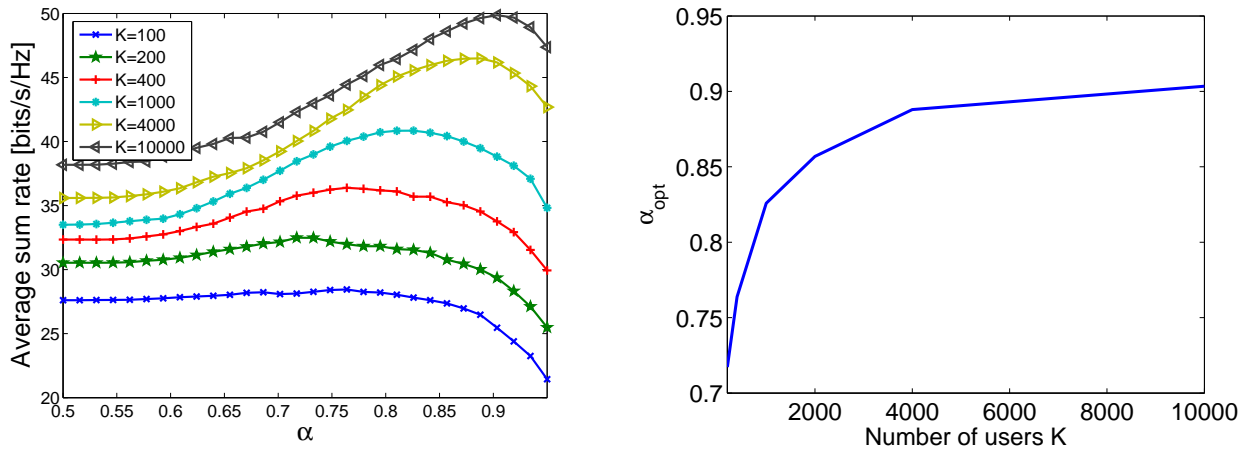


Fig. 6. Multi-group performance: (a) sum rate w.r.t. α and (b) optimal α

SUS-ZFBF requires the largest amount of feedback. Note that the amount of feedback required for ReDOS-PBR is even less than RBF! We then investigated the performance sensitivity of ReDOS-PBR w.r.t. α in the same setting as in Fig. 5, and the result is shown in Fig. 6. It is seen that optimal α increases as K increases. An observation of practical importance is that the performance of ReDOS-PBR is quite insensitive w.r.t. α for the practical range of the number of users.

Next, we considered a single-group case for which SUS-ZFBF is originally proposed. The

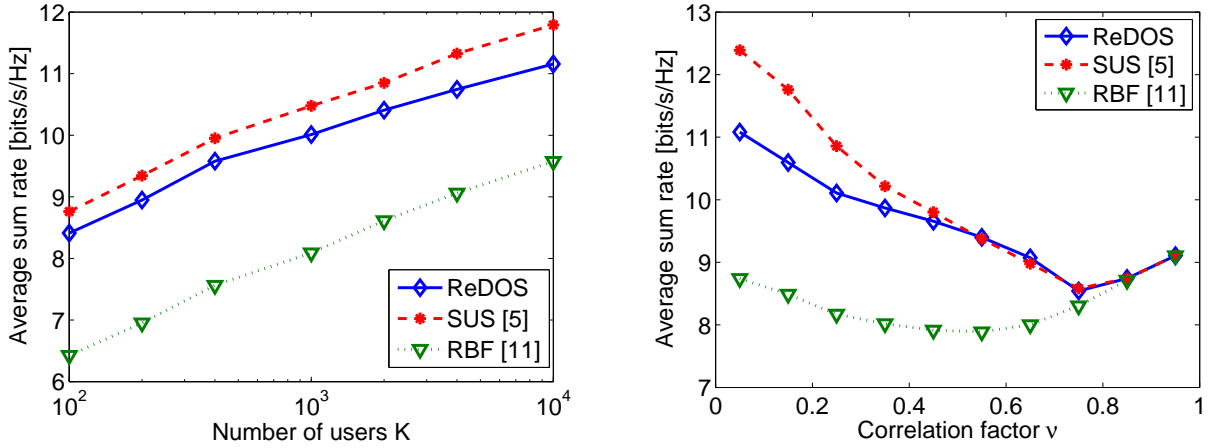


Fig. 7. Single-group performance: (a) average sum rate w.r.t. K and (b) average sum rate w.r.t. the channel correlation factor ν

considered system consists of a BS with $M = r_g^* = 4$ and $P = 10$ [dB], and K UTs each with a single antenna. The channel vector for each user was generated i.i.d. according to the model (1), where for the channel covariance matrix \mathbf{R}_1 , the exponential correlation model is used, i.e., [11]

$$[\mathbf{R}_1]_{i,j} = \nu^{|i-j|} \quad (59)$$

with $0 \leq \nu \leq 1$. Fig. 7 (a) shows the average sum-rate performance of SUS-ZFBF, RBF and ReDOS-PBR for $\nu = 0.3$. Again, there exists a significant performance gap between SUS-ZFBF and RBF, and ReDOS-PBR closely follows SUS-ZFBF. Fig. 7 (b) shows the performance of the three schemes w.r.t. the channel correlation factor ν with K fixed to 1000 for the same setting as in Fig. 7 (a). As expected, when $\nu = 0$, i.e., the channel is isotropic, SUS-ZFBF performs best, and when $\nu = 1$, i.e., the channel matrix has rank one and only one beam can be supported, all three algorithms perform equally. It is seen that the noticeable gap between SUS-ZFBF and ReDOS-PBR at $\nu = 0$ decreases as ν increases towards one. This is because when the channel becomes more correlated, there start to exist dominant eigen-directions of the channel and thus, it is enough to make these dominant eigen-directions of the channel the reference beam directions of ReDOS-PBR and to look around these reference directions.

Finally, we examined the performance of ReDOS-PBR-PF. We considered two ReDOS-PBR-PF algorithms: One with fixed $\alpha = \alpha_{min}$ for all users and the other with adaptive α for each

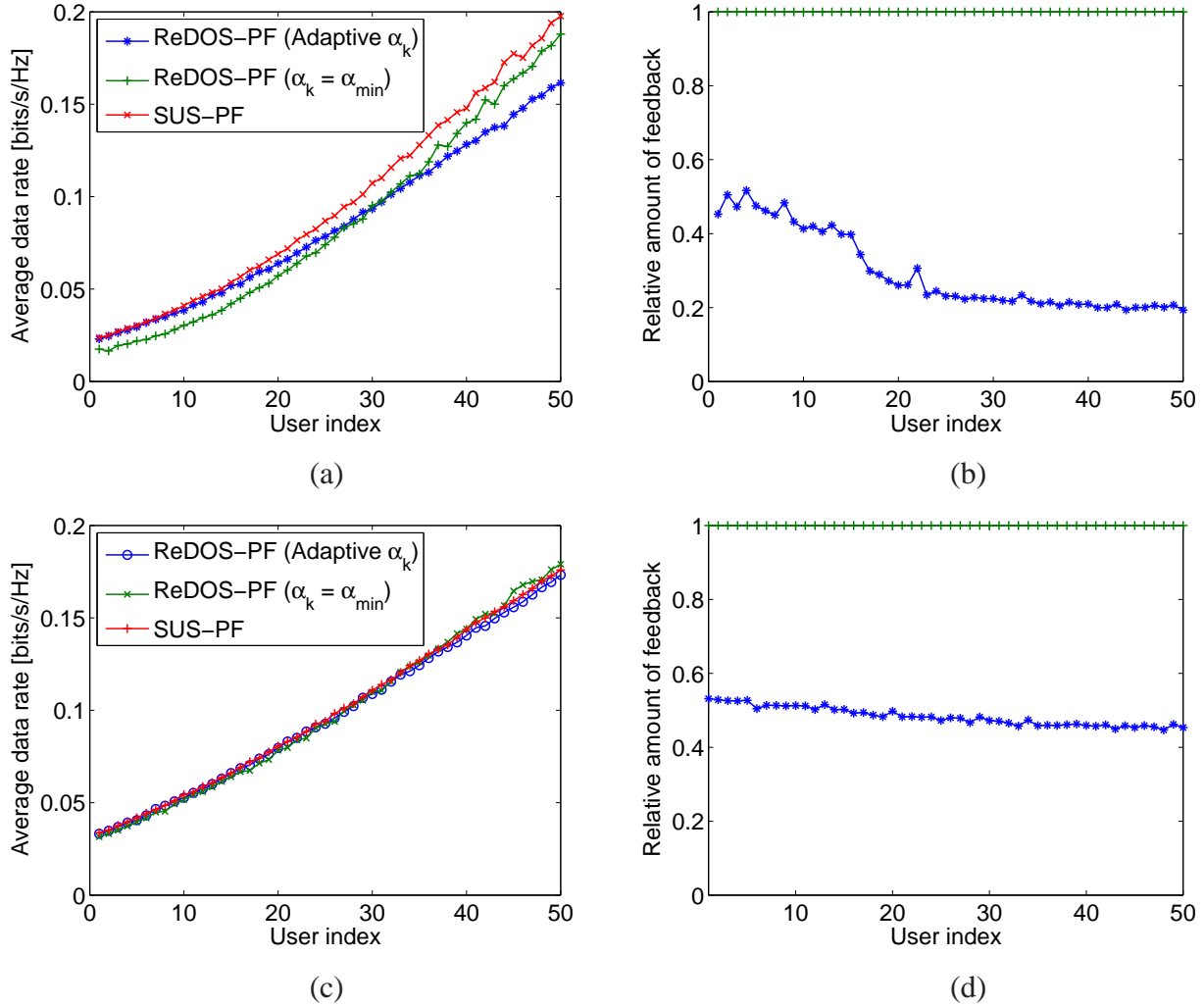


Fig. 8. Performance of ReDOS-PBR-PF: (a) each user's served rate, (b) relative amount of feedback between two ReDOS-PBR-PF algorithms: one with fixed α and the other with adaptive α , (c) each user's served rate, and (d) relative amount of feedback between two ReDOS-PBR-PF algorithms ((a) and (b): $\nu = 0.1$ and $\Delta_{\alpha,up} = 0.1$ and $\Delta_{\alpha,down} = \Delta_{\alpha,up}/50$, and (c) and (d): $\nu = 0.3$ and $\Delta_{\alpha,up} = 0.2$ and $\Delta_{\alpha,down} = \Delta_{\alpha,up}/100$)

user with steps $\Delta_{\alpha,up}$ and $\Delta_{\alpha,down}$ described in Algorithm 3. To simplify the simulation, we just considered the single-group system considered in Fig. 7. Here, we fixed $K = 50$ and BS $P = 0$ [dB]. The channel vector for each user k was generated as

$$\mathbf{h}_k \sim \sqrt{l_k} \mathbf{R}_1^{1/2} \boldsymbol{\eta}_k, \quad (60)$$

where \mathbf{R}_1 is given in (59); $\boldsymbol{\eta}_k \stackrel{i.i.d.}{\sim} \mathcal{CN}(\mathbf{0}, \mathbf{I}_4)$; and the large-scale fading effect is captured in l_k . The large-scale fading factor l_k for 50 users were designed such that the lowest power user has

$l_k = 1$ and the highest power user has $l_k = 100$ (20 dB difference), and other users' power is equally spaced in dB scale in the 20 dB power range. We ran 10,000 scheduling intervals. For each interval, the channel vector for each user was generated independently as described in the above. Fig. 8 (a) shows the average served rate for 50 users (users are ordered in an ascending order of their l_k values) over 10,000 scheduling intervals, when the channel is almost isotropic, i.e., $\nu = 0.1$. It is seen in this case that there is some loss of ReDOS-PBR-PF compared to SUS-ZFBF-PF. Note that ReDOS-PBR-PF with fixed $\alpha = \alpha_{min}$ tracks SUS-ZFBF-PF for all users with equal gap, but ReDOS-PBR-PF with adaptive α sacrifices high-SNR users and gives more chances to low-SNR users. (This is evident in Fig. 8 (b).) This is because high-SNR users have more chances to be selected and thus, increase their α_k to reduce this increased chance. Fig. 8 (b) shows the relative amount of feedback for ReDOS-PBR-PF with adaptive α to that of ReDOS-PBR-PF with fixed α . It is seen that the amount of feedback is significantly reduced by adapting α . Figs. (c) and (d) show the performance and the relative amount of feedback in the case of $\nu = 0.3$. It is seen that when the channel correlation increases, the performance difference between ReDOS-PBR-PF and SUS-ZFBF-PF is negligible.

VII. CONCLUSION

In this paper, we have proposed a new efficient user-scheduling-and-beamforming method for massive MU-MIMO broadcast channels. The proposed method takes advantage of two existing user-scheduling-and-beamforming methods, SUS-ZFBF and RBF, for MU-MIMO broadcast channels sitting on opposite sides on the scale of feedback overhead. The proposed scheduling-and-beamforming method is asymptotically optimal as the number of users increases. The proposed method yields 'nearly-optimal' user-selection-and-beamforming under the linear beamforming framework for MU-MIMO downlink, based on CQI-only feedback from possibly all users and CSI feedback from only the scheduled users.

APPENDIX A

INNER PRODUCT BETWEEN TWO VECTORS IN TWO DIFFERENT CONES

Lemma 2: For two channel vectors contained in two different user-selection cones, i.e., $\mathbf{h}_{\kappa_{g,i}} \in \mathcal{C}_{g,i}$ and $\mathbf{h}_{\kappa_{g,j}} \in \mathcal{C}_{g,j}$, $i \neq j$, the inner product between the corresponding normalized effective

channel vectors $\tilde{\mathbf{g}}_{\kappa_{g,i}}$ and $\tilde{\mathbf{g}}_{\kappa_{g,j}}$ with norm one is bounded by

$$|\tilde{\mathbf{g}}_{\kappa_{g,i}}^H \tilde{\mathbf{g}}_{\kappa_{g,j}}| \leq 2\alpha\sqrt{1-\alpha^2} \quad \text{for } i \neq j, \quad (61)$$

when $\alpha \geq 1/\sqrt{2}$ (i.e., the angle $\theta \leq \pi/4$ in Fig. 3).

Proof: Let $\tilde{\mathbf{g}}_{\kappa_{g,i}} = \sum_{m=1}^{r_g^*} c_{\kappa_{g,i}}^m \mathbf{e}_m^{(g)}$ and $\tilde{\mathbf{g}}_{\kappa_{g,j}} = \sum_{m=1}^{r_g^*} c_{\kappa_{g,j}}^m \mathbf{e}_m^{(g)}$, where $\mathbf{e}_m^{(g)}$ is the m -th column of $\mathbf{I}_{r_g^*}$. Then, we have $\sum_m |c_{\kappa_{g,i}}^m|^2 = \sum_m |c_{\kappa_{g,j}}^m|^2 = 1$ and

$$\begin{aligned} |\tilde{\mathbf{g}}_{\kappa_{g,i}}^H \tilde{\mathbf{g}}_{\kappa_{g,j}}| &= \left| \sum_{m=1}^{r_g^*} \bar{c}_{\kappa_{g,i}}^m c_{\kappa_{g,j}}^m \right| \\ &\leq \sum_{m=1}^{r_g^*} |\bar{c}_{\kappa_{g,i}}^m| \cdot |c_{\kappa_{g,j}}^m| \\ &= |\bar{c}_{\kappa_{g,i}}^i| \cdot |c_{\kappa_{g,j}}^i| + |\bar{c}_{\kappa_{g,i}}^j| \cdot |c_{\kappa_{g,j}}^j| + \sum_{m=1, m \neq i, j}^{r_g^*} |\bar{c}_{\kappa_{g,i}}^m| |c_{\kappa_{g,j}}^m| \\ &\leq |\bar{c}_{\kappa_{g,i}}^i| \cdot |c_{\kappa_{g,j}}^i| + |\bar{c}_{\kappa_{g,i}}^j| \cdot |c_{\kappa_{g,j}}^j| + \left(\sum_{m=1, m \neq i, j}^{r_g^*} |\bar{c}_{\kappa_{g,i}}^m|^2 \right)^{\frac{1}{2}} \left(\sum_{m=1, m \neq i, j}^{r_g^*} |c_{\kappa_{g,j}}^m|^2 \right)^{\frac{1}{2}}, \quad (62) \end{aligned}$$

where \bar{c} is the complex conjugate of c , and the last step follows from the Cauchy-Schwarz inequality.

Now consider the RHS in (62). First, fix $\{c_{\kappa_{g,j}}^m\}_{m=1}^{r_g^*}$ and $|\bar{c}_{\kappa_{g,i}}^i|$, and view the RHS in (62) as a function of $\{c_{\kappa_{g,i}}^m, m = 1, \dots, r_g^* \text{ and } m \neq i \mid \sum_{m=1, m \neq i}^{r_g^*} |c_{\kappa_{g,i}}^m|^2 = 1 - |c_{\kappa_{g,i}}^i|^2\}$. Then, the RHS in (62) is in the form of $a + bx + cy$, where the constants $a, b, c \geq 0$ are given by $a = |\bar{c}_{\kappa_{g,i}}^i| \cdot |c_{\kappa_{g,j}}^i|$, $b = |c_{\kappa_{g,j}}^j|$, and $c = \left(\sum_{m=1, m \neq i, j}^{r_g^*} |c_{\kappa_{g,j}}^m|^2 \right)^{\frac{1}{2}}$, and the variables $x, y \geq 0$ are given by $x = |\bar{c}_{\kappa_{g,i}}^j|$ and $y = \sum_{m=1, m \neq i, j}^{r_g^*} |\bar{c}_{\kappa_{g,i}}^m|^2$, with a constraint $x^2 + y^2 = 1 - |\bar{c}_{\kappa_{g,i}}^i|^2$. This convex optimization is solved by using the Karush-Kuhn-Tucker conditions [25], and the solution is given by

$$x = b \sqrt{\frac{1 - |c_{\kappa_{g,i}}^i|^2}{1 - |c_{\kappa_{g,j}}^i|^2}} \quad \text{and} \quad y = c \sqrt{\frac{1 - |c_{\kappa_{g,i}}^i|^2}{1 - |c_{\kappa_{g,j}}^i|^2}}. \quad (63)$$

Substituting this x, y into the RHS of (62), we have

$$\begin{aligned} |\tilde{\mathbf{g}}_{\kappa_{g,i}}^H \tilde{\mathbf{g}}_{\kappa_{g,j}}| &\leq a + bx + cy = a + (b^2 + c^2) \sqrt{\frac{1 - |c_{\kappa_{g,i}}^i|^2}{1 - |c_{\kappa_{g,j}}^i|^2}} \\ &\stackrel{(a)}{=} |c_{\kappa_{g,i}}^i| \cdot |c_{\kappa_{g,j}}^i| + \sqrt{1 - |c_{\kappa_{g,i}}^i|^2} \cdot \sqrt{1 - |c_{\kappa_{g,j}}^i|^2} \quad (64) \end{aligned}$$

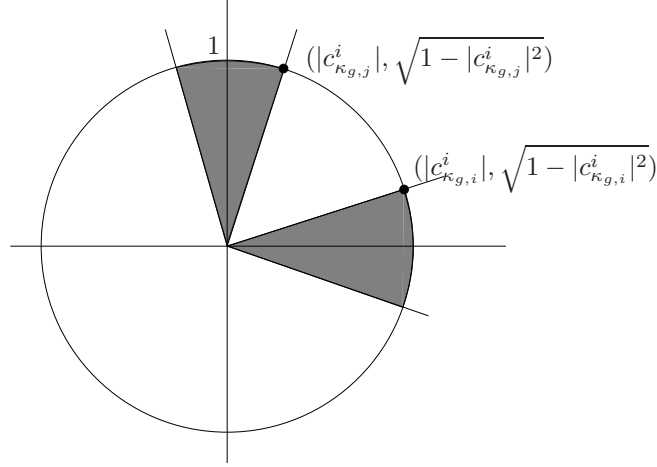


Fig. 9. Maximum inner product between two cones

where (a) follows from $b^2 + c^2 = 1 - |c_{\kappa_g,j}^i|^2$. Now, the RHS in (64) is expressed in terms of $|c_{\kappa_g,i}^i|$ and $|c_{\kappa_g,j}^i|$ which comprised the constant term a in the previous optimization of $a + bx + cy$. Here, we have the following conditions for the terms in the RHS in (64):

$$|c_{\kappa_g,i}^i| \geq \alpha \quad (65)$$

$$\sqrt{1 - |c_{\kappa_g,i}^i|^2} \leq \sqrt{1 - \alpha^2} \quad (66)$$

$$|c_{\kappa_g,j}^i| = \sqrt{1 - \sum_{m=1, m \neq i}^{r_g^*} |c_{\kappa_g,j}^m|^2} \leq \sqrt{1 - |c_{\kappa_g,j}^j|^2} \leq \sqrt{1 - \alpha^2} \quad (67)$$

$$\sqrt{1 - |c_{\kappa_g,j}^i|^2} \geq \alpha, \quad (68)$$

where (65) is valid by the cone-containment condition. The RHS in (64) is the inner product between two points $(|c_{\kappa_g,i}^i|, \sqrt{1 - |c_{\kappa_g,i}^i|^2})$ and $(|c_{\kappa_g,j}^i|, \sqrt{1 - |c_{\kappa_g,j}^i|^2})$ with constraints (65) to (68). The situation is depicted in Fig. 9. The maximum inner product occurs between $(\alpha, \sqrt{1 - \alpha^2})$ and $(\sqrt{1 - \alpha^2}, \alpha)$ and is given by $2\alpha\sqrt{1 - \alpha^2}$. Therefore, we have

$$|\tilde{\mathbf{g}}_{\kappa_g,i}^H \tilde{\mathbf{g}}_{\kappa_g,j}| \leq 2\alpha\sqrt{1 - \alpha^2} \quad \text{for } i \neq j. \quad (69)$$

Without the condition $\alpha \geq 1/\sqrt{2}$, the two shaded regions in Fig. 9 overlap, and we have a trivial upper bound of one. ■

APPENDIX B

BASIC EXTREME VALUE THEORY

First, we present two required theorems regarding the asymptotic behavior of the maximum of K i.i.d. random variables when K increases without bound.

Theorem 3: ([26]–[28]) Let Z_1, \dots, Z_K be i.i.d. random variables with a common cumulative density function (CDF) $F(\cdot)$. Suppose that there exist sequences $\{a_i > 0\}_{i=1}^K$ and $\{b_i\}_{i=1}^K$ of normalizing constants such that

$$\lim_{K \rightarrow \infty} F^K(a_K z + b_K) = G(z), \quad (70)$$

where $F^K(\cdot)$ is $F(\cdot)$ to the power of K . Then, $G(z)$ must be one of the following three types of functions:

$$(i) \quad G_1(z) = \begin{cases} 0, & z \leq 0 \\ e^{-z^{-\alpha}}, & z > 0, \alpha > 0 \end{cases} \quad (71)$$

$$(ii) \quad G_2(z) = \begin{cases} e^{-(z)^{\alpha}}, & z \leq 0, \alpha > 0 \\ 1, & z > 0 \end{cases} \quad (72)$$

$$(iii) \quad G_3(z) = e^{-e^{-z}}. \quad (73)$$

Theorem 4: ([27], [29]) For distribution function F^K and $G_l(z)$, we have

$$\lim_{K \rightarrow \infty} F^K(a_K z + b_K) = G_l(z) \quad (74)$$

if and only if

$$\lim_{K \rightarrow \infty} K[1 - F(a_K z + b_K)] = -\log[G_l(z)], \quad (75)$$

where $l \in \{1, 2, 3\}$, for two sequences $\{a_i > 0\}_{i=1}^K$ and $\{b_i\}_{i=1}^K$.

Definition 1 (Generalized chi-square distribution [30]): If $X_i \stackrel{i.i.d.}{\sim} \mathcal{CN}(0, 1)$ for $i = 1, \dots, L$, then the variable $\chi_{\text{Gen}}^2(\lambda_1, \dots, \lambda_L) := \sum_{i=1}^L \lambda_i |X_i|^2$ with $\lambda_1 > \lambda_2 > \dots > \lambda_L > 0$ is called a generalized chi-square random variable with order L and parameters $\lambda_1, \lambda_2, \dots, \lambda_L$. Then, $\chi_{\text{Gen}}^2(\lambda_1, \dots, \lambda_L)$ has the pdf

$$f_{\chi_{\text{Gen}}^2}(z) = \sum_{i=1}^L \frac{e^{-z/\lambda_i}}{\lambda_i \prod_{j=1, j \neq i}^L (1 - \frac{\lambda_j}{\lambda_i})}, \quad \text{for } z \geq 0. \quad (76)$$

Furthermore, its CDF is given by

$$F_{\chi_{\text{Gen}}^2}(z) = \sum_{i=1}^L \frac{1 - e^{-z/\lambda_i}}{\xi_i} \quad \text{and} \quad \sum_{i=1}^L \frac{1}{\xi_i} = 1, \quad (77)$$

where

$$\xi_i = \prod_{j=1, j \neq i}^L \left(1 - \frac{\lambda_j}{\lambda_i}\right). \quad (78)$$

Now, in a way similar to the technique used in [29], we further generalize the generalized chi-square distribution, and define a generalized CDF^{††} from the CDF of $\chi_{\text{Gen}}^2(\lambda_1, \dots, \lambda_L)$:

$$F(z) = \begin{cases} 1 - \zeta \sum_{i=1}^L \frac{e^{-z/\lambda_i}}{\xi_i}, & z \geq z_\tau, \\ \tilde{F}(z), & z < z_\tau, \end{cases} \quad (79)$$

for $0 < \zeta < 1$ is a fixed constant, $z_\tau (< \infty)$ is a fixed finite threshold, and $\tilde{F}(z)$ is an arbitrary monotone-increasing continuous function satisfying $\tilde{F}(0) = 0$ and $\tilde{F}(z_\tau) = 1 - \zeta \sum_{i=1}^L \frac{e^{-z_\tau/\lambda_i}}{\xi_i}$. Then, this is a valid CDF over $z \geq 0$ since $F(0) = 0$, $F(\infty) = 1$, and $F(z)$ is continuous and monotone increasing. Based on the two theorems in the above, we derive the following lemma regarding the newly defined CDF in (79), necessary for proof of (51, 52).

Lemma 3: Let Z_1, Z_2, \dots, Z_K be K i.i.d. random variables with the CDF in (79) with $\lambda_1 > \lambda_2 > \dots > \lambda_L$. Then, the limiting behavior of F^K belongs to type (iii) in Theorem 3 with normalizing sequences

$$a_K = \lambda_1, \quad b_K = \lambda_1(\log K + \log(\zeta/\xi_1)), \quad (80)$$

and therefore, we have

$$\Pr\{Z_{\max} > \lambda_1 \log K - \lambda_1 \log \log K + \lambda_1 \log(\zeta/\xi_1)\} \geq 1 - O\left(\frac{1}{K}\right), \quad (81)$$

where Z_{\max} denotes the maximum of $\{Z_i\}_{i=1}^K$.

^{††}In extreme value theory, typically the maximum of i.i.d. random variables is considered and thus, only the upper tail behavior of the CDF matters [26]–[28].

Proof: Compute $K[1 - F(a_K z + b_K)]$ with a_K and b_K in (80) when $a_K z + b_K \geq z_\tau$:

$$\lim_{K \rightarrow \infty} K[1 - F(a_K z + b_K)] = \lim_{K \rightarrow \infty} K \zeta \left[\sum_{i=1}^L \frac{e^{-(a_K z + b_K)/\lambda_i}}{\xi_i} \right] \quad (82)$$

$$= \lim_{K \rightarrow \infty} K \zeta \left[\sum_{i=1}^L \frac{e^{-[z + \log K + \log(\zeta/\xi_1)] \frac{\lambda_1}{\lambda_i}}}{\xi_i} \right] \quad (83)$$

$$= \lim_{K \rightarrow \infty} K \left[\frac{e^{-z}}{K} + \zeta \sum_{i=2}^L \frac{[e^{-z}(\xi_1/\zeta)]^{\frac{\lambda_1}{\lambda_i}}}{\xi_i K^{\frac{\lambda_1}{\lambda_i}}} \right] \quad (84)$$

$$\stackrel{(a)}{=} e^{-z} = -\log[G_3(z)], \quad (85)$$

where (a) follows from the fact that $\frac{\lambda_1}{\lambda_i} > 1$ for $i = 2, \dots, L$, and the second term in the RHS of (84) vanishes as $K \rightarrow \infty$. By Theorems 3 and 4, the limiting behavior of F^K belongs to type (iii) in Theorem 3 with the normalizing sequences a_K and b_K in (80), when $a_K z + b_K \geq z_\tau$ for sufficiently large K . Hence, we have

$$\lim_{K \rightarrow \infty} F^K(\lambda_1 z + \lambda_1 \log K + \lambda_1 \log(\zeta/\xi_1)) = e^{-e^{-z}}, \quad (86)$$

when $a_K z + b_K \geq z_\tau$ for sufficiently large K . This implies

$$\lim_{K \rightarrow \infty} \Pr\{Z_{\max} > \lambda_1 z + \lambda_1 \log K + \lambda_1 \log(\zeta/\xi_1)\} = 1 - e^{-e^{-z}}, \quad (87)$$

because F^K is the CDF of $Z_{\max} = \max\{Z_1, \dots, Z_K\}$. By substituting $z = -\log \log K$ and removing the limit operator, we get

$$\Pr\{Z_{\max} > \lambda_1 \log K - \lambda_1 \log \log K + \lambda_1 \log(\zeta/\xi_1)\} \geq 1 - O\left(\frac{1}{K}\right) \quad (88)$$

since $a_K z + b_K \geq z_\tau$ for sufficiently large K with $z = -\log \log K$ and (a_K, b_K) in (80) due to the term “ $\log K$ ” in b_K . ■

APPENDIX C

PROOF OF (51, 52)

Now we prove (51, 52) in the proof of Theorem 2 under the conditions of Theorem 2. The impact of no quasi-SINR feedback by the users whose channel vectors are not contained in the user-selection cones, is incorporated by defining $\phi_{g_k}^i$ in (49). To handle the inter-group

interference, we here define new random variables. For each $i \in \{1, \dots, r_g^*\}$, we define random variables $\bar{\phi}_{g_k}^i$, $k = 1, \dots, K'$, as

$$\bar{\phi}_{g_k}^i = \begin{cases} \phi_{g_k}^i, & k \in \mathcal{V}_g(\epsilon) \\ 0, & \text{otherwise} \end{cases} \quad (89)$$

where

$$\mathcal{V}_g(\epsilon) := \left\{ k : \sum_{g' \neq g} \|\mathbf{h}_{g_k}^H \mathbf{V}_{g'}\|^2 \leq \frac{\epsilon}{r_g^*} \right\} \quad (90)$$

for some constant $\epsilon > 0$. Let us define the following sets:

$$\overline{\mathcal{W}}_{g,i}(\alpha) := \{\mathbf{h}_{g_k} : k \in \mathcal{W}_{g,i}(\alpha)\}, \quad i \in \{1, \dots, r_g^*\} \quad (91)$$

$$\overline{\mathcal{V}}_g(\epsilon) := \{\mathbf{h}_{g_k} : k \in \mathcal{V}_g(\epsilon)\}, \quad (92)$$

where $\mathcal{W}_{g,i}(\alpha)$ is defined in Algorithm 1. (The dependence of $\mathcal{W}_{g,i}$ on α is explicitly shown here.

$\overline{\mathcal{W}}_{g,i}(\alpha)$ and $\overline{\mathcal{V}}_g(\epsilon)$ are simply denoted by $\overline{\mathcal{W}}_{g,i}$ and $\overline{\mathcal{V}}_g$, respectively, in case of no confusion.)

Note that the fixed and chosen $\bar{\alpha}$ satisfies

$$\bar{\alpha} > \sqrt{\frac{1 + \sqrt{\frac{r_g^* - 2}{r_g^* - 1}}}{2}}, \quad (93)$$

and this implies $\alpha > \frac{1}{\sqrt{2}}$ for any $r_g^* \geq 2$. Then, the user-selection cones are disjoint (see Remark 5) and hence, we can rewrite $\overline{\mathcal{W}}_{g,i}$ as

$$\overline{\mathcal{W}}_{g,i} = \left\{ \mathbf{h}_{g_k} : \frac{|(\mathbf{h}_{g_k}^H \mathbf{V}_g) \mathbf{e}_i^{(g)}|^2}{\|\mathbf{h}_{g_k}^H \mathbf{V}_g\|^2} \geq \alpha^2 \right\}, \quad \because \mathbf{g}_{g_k}^H = \mathbf{h}_{g_k}^H \mathbf{V}_g = \mathbf{h}_{g_k}^H \mathbf{U}_g^* \quad (94)$$

$$= \left\{ \mathbf{h}_{g_k} : \frac{\lambda_{g,i} |\eta_{g_k,i}|^2}{\sum_{m=1}^{r_g^*} \lambda_{g,m} |\eta_{g_k,m}|^2} \geq \alpha^2 \right\}, \quad i = 1, \dots, r_g^*, \quad (95)$$

where $\lambda_{g,i}$ is the i -th largest eigenvalue of \mathbf{R}_g , and $\eta_{g_k,m}$ is the m -th element of $\boldsymbol{\eta}_{g_k}$ given in the channel model (1~4). This is because from (1~4)

$$\begin{aligned} \mathbf{h}_{g_k} &= \mathbf{U}_g \boldsymbol{\Lambda}_g^{1/2} \boldsymbol{\eta}_{g_k} = \sum_{i=1}^{r_g} \eta_{g_k,i} \sqrt{\lambda_{g,i}} \mathbf{u}_{g,i}, \\ \mathbf{g}_{g_k}^H &= \mathbf{h}_{g_k}^H \mathbf{V}_g = \mathbf{h}_{g_k}^H \mathbf{U}_g^*, \\ &= [\eta_{g_k,1}^* \sqrt{\lambda_{g,1}}, \eta_{g_k,2}^* \sqrt{\lambda_{g,2}}, \dots, \eta_{g_k,r_g^*}^* \sqrt{\lambda_{g,r_g^*}}]. \end{aligned} \quad (96)$$

Now consider $\bar{\mathcal{V}}_g$ in (92). This set can be rewritten as

$$\bar{\mathcal{V}}_g = \left\{ \mathbf{h}_{g_k} : \sum_{g' \neq g} \|\mathbf{h}_{g_k}^H \mathbf{V}_{g'}\|^2 \leq \frac{\epsilon}{r_g^*} \right\} \quad (97)$$

$$= \left\{ \mathbf{h}_{g_k} : \sum_{g' \neq g} \|\eta_{g_k}^H \Lambda^{1/2} \underbrace{\mathbf{U}_g^H \mathbf{V}_{g'}}_{\text{see (100)}}\|^2 \leq \frac{\epsilon}{r_g^*} \right\}, \quad (\mathbf{V}_{g'} = \mathbf{U}_{g'}^*) \quad (98)$$

$$\stackrel{(a)}{=} \left\{ \mathbf{h}_{g_k} : \sum_{g' \neq g} \left\| \sum_{m=r_g^*+1}^{r_g} \eta_{g_k, m} \sqrt{\lambda_{g, m}} \mathbf{x}_{g, g'}^{(m)} \right\|^2 \leq \frac{\epsilon}{r_g^*} \right\}. \quad (99)$$

Step (a) is by the approximate BD condition in Condition 1 assumed for Theorem 2, i.e., [12]

$$\mathbf{U}_g^H \mathbf{V}_{g'} = \mathbf{U}_g^H \mathbf{U}_{g'}^* = \begin{bmatrix} \mathbf{0}_{r_g^* \times r_{g'}^*} \\ \mathbf{X}_{g, g'} \end{bmatrix}, \quad (100)$$

where $\mathbf{X}_{g, g'}$ is some matrix of size $(r_g - r_g^*) \times r_{g'}^*$ which can be a non-zero matrix, and $\mathbf{x}_{g, g', m}$ in (99) is the m -th row vector of $\mathbf{U}_g^H \mathbf{V}_{g'}$. One key observation regarding $\bar{\mathcal{W}}_{g, i}$ and $\bar{\mathcal{V}}_g$ is that the event of $\mathbf{h}_{g_k} \in \bar{\mathcal{W}}_{g, i}$ and the event of $\mathbf{h}_{g_k} \in \bar{\mathcal{V}}_g$ are independent under the approximate BD condition, because the former event depends only on $\{\eta_{g_k, 1}, \dots, \eta_{g_k, r_g^*}\}$, the latter event depends only on $\{\eta_{g_k, r_g^*+1}, \dots, \eta_{g_k, r_g}\}$, and the random variables $\eta_{g_k, 1}, \eta_{g_k, 2}, \dots, \eta_{g_k, r_g}$ are i.i.d. (Please see (4).)

Now, we obtain a lower bound on the complementary CDF (CCDF) of $\phi_{g_k}^i$ of user g_k :

$$\begin{aligned} \Pr\{\phi_{g_k}^i \geq z\} &\geq \Pr\{\bar{\phi}_{g_k}^i \geq z\} \\ &\stackrel{(a)}{=} \Pr\{\bar{\phi}_{g_k}^i \geq z, \mathbf{h}_{g_k} \in \bar{\mathcal{W}}_{g, i}, \mathbf{h}_{g_k} \in \bar{\mathcal{V}}_g\} \\ &= \Pr\{\mathbf{h}_{g_k} \in \bar{\mathcal{W}}_{g, i}, \mathbf{h}_{g_k} \in \bar{\mathcal{V}}_g\} \cdot \Pr\{\bar{\phi}_{g_k}^i \geq z | \mathbf{h}_{g_k} \in \bar{\mathcal{W}}_{g, i}, \mathbf{h}_{g_k} \in \bar{\mathcal{V}}_g\} \\ &\stackrel{(b)}{=} \Pr\{\mathbf{h}_{g_k} \in \bar{\mathcal{W}}_{g, i}, \mathbf{h}_{g_k} \in \bar{\mathcal{V}}_g\} \Pr\left\{ \frac{\|\mathbf{g}_{g_k}\|^2}{\frac{1}{\rho} + r_g^* \sum_{g' \neq g} \|\mathbf{h}_{g_k}^H \mathbf{V}_{g'}\|^2} \geq z \middle| \mathbf{h}_{g_k} \in \bar{\mathcal{W}}_{g, i}, \mathbf{h}_{g_k} \in \bar{\mathcal{V}}_g \right\} \\ &\stackrel{(c)}{\geq} \Pr\{\mathbf{h}_{g_k} \in \bar{\mathcal{W}}_{g, i}, \mathbf{h}_{g_k} \in \bar{\mathcal{V}}_g\} \Pr\left\{ \frac{\|\mathbf{g}_{g_k}\|^2}{\frac{1}{\rho} + \epsilon} \geq z \middle| \mathbf{h}_{g_k} \in \bar{\mathcal{W}}_{g, i}, \mathbf{h}_{g_k} \in \bar{\mathcal{V}}_g \right\} \\ &\stackrel{(d)}{=} \Pr\{\mathbf{h}_{g_k} \in \bar{\mathcal{W}}_{g, i}, \mathbf{h}_{g_k} \in \bar{\mathcal{V}}_g\} \Pr\left\{ \frac{\|\mathbf{g}_{g_k}\|^2}{\frac{1}{\rho} + \epsilon} \geq z \middle| \mathbf{h}_{g_k} \in \bar{\mathcal{W}}_{g, i} \right\} \\ &\stackrel{(e)}{=} \Pr\{\mathbf{h}_{g_k} \in \bar{\mathcal{W}}_{g, i}\} \Pr\{\mathbf{h}_{g_k} \in \bar{\mathcal{V}}_g\} \Pr\left\{ \frac{\|\mathbf{g}_{g_k}\|^2}{\frac{1}{\rho} + \epsilon} \geq z \middle| \mathbf{h}_{g_k} \in \bar{\mathcal{W}}_{g, i} \right\} \\ &\stackrel{(f)}{\geq} \Pr\{\mathbf{h}_{g_k} \in \bar{\mathcal{W}}_{g, i}\} \Pr\{\mathbf{h}_{g_k} \in \bar{\mathcal{V}}_g\} \Pr\{\|\mathbf{g}_{g_k}\|^2 \geq z'\}, \quad z' = z(1/\rho + \epsilon). \end{aligned} \quad (101)$$

Here, (a) is because the events $\{\bar{\phi}_{g_k}^i \geq z\}$ and $\{\bar{\phi}_{g_k}^i \geq z, \mathbf{h}_{g_k} \in \overline{\mathcal{W}}_{g,i}, \mathbf{h}_{g_k} \in \overline{\mathcal{V}}_g\}$ are the same for $z > 0$ due to the definition of $\bar{\phi}_{g_k}^i$; (b) follows because conditioned on $\{\mathbf{h}_{g_k} \in \overline{\mathcal{W}}_{g,i}, \mathbf{h}_{g_k} \in \overline{\mathcal{V}}_g\}$, $\bar{\phi}_{g_k}^i = \mathcal{R}(g_k)$; (c) is valid because conditioned on $\{\mathbf{h}_{g_k} \in \overline{\mathcal{V}}_g\}$, $\mathcal{R}(g_k) \geq \|\mathbf{g}_{g_k}\|^2/(1/\rho + \epsilon)$; (d) is valid because the events $\{\mathbf{h}_{g_k} \in \overline{\mathcal{W}}_{g,i}\}$ and $\{\mathbf{h}_{g_k} \in \overline{\mathcal{V}}_g\}$ are independent, and the event $\frac{\|\mathbf{g}_{g_k}\|^2}{1/\rho + \epsilon} \geq z$ is independent of $\{\mathbf{h}_{g_k} \in \overline{\mathcal{V}}_g\}$; (e) is valid because the events $\{\mathbf{h}_{g_k} \in \overline{\mathcal{W}}_{g,i}\}$ and $\{\mathbf{h}_{g_k} \in \overline{\mathcal{V}}_g\}$ are independent; and finally (f) follows from Lemma 4.

For given $\alpha < 1$ and $\epsilon > 0$, define $\zeta_{g,i}(\alpha, \epsilon)$ as

$$\zeta_{g,i}(\alpha, \epsilon) := \Pr\{\mathbf{h}_{g_k} \in \overline{\mathcal{W}}_{g,i}(\alpha)\} \Pr\{\mathbf{h}_{g_k} \in \overline{\mathcal{V}}_g(\epsilon)\} > 0. \quad (102)$$

Note that $\zeta_{g,i}(\alpha, \epsilon) \in (0, 1)$ is a positive constant, when $\alpha < 1$ and $\epsilon > 0$ are given, since we have a strictly positive probability for the event $\{\mathbf{h}_{g_k} \in \overline{\mathcal{W}}_{g,i}(\alpha)\}$ and a strictly positive probability for $\{\mathbf{h}_{g_k} \in \overline{\mathcal{V}}_g(\epsilon)\}$. Now, we define new i.i.d. random variables Ψ_{g_k} for $k = 1, \dots, K'$ that have the common complementary CDF (CCDF) constructed as

$$\Pr\{\Psi_{g_k} \geq z\} = \begin{cases} \zeta_{g,i}(\alpha, \epsilon) \cdot \Pr\{\|\mathbf{g}_{g_k}\|^2 \geq z\}, & z \geq z_\tau, \\ \tilde{F}_C(z), & z < z_\tau, \end{cases} \quad (103)$$

where $\tilde{F}_C(z)$ is constructed arbitrarily such that (103) is a CCDF. Then, the corresponding CDF of (103) is given by

$$F(z) = \begin{cases} 1 - \zeta_{g,i}(\alpha, \epsilon) \sum_{j=1}^{r_g^*} \frac{e^{-z/\lambda_{g,j}}}{\xi_{g,j}}, & z \geq z_\tau \\ 1 - \tilde{F}_C(z), & z < z_\tau, \end{cases} \quad (104)$$

since $\|\mathbf{g}_{g_k}\|^2$ is $\chi_{\text{Gen}}^2(\lambda_{g,1}, \dots, \lambda_{g,r_g^*})$ defined in Definition 1 (see (96)), where the parameters $\lambda_{g,1}, \dots, \lambda_{g,r_g^*}$ are the eigenvalues of the channel covariance matrix \mathbf{R}_g in the channel model (1 ~ 4). The CDF (104) falls into the CDF class of (79) and hence, we can apply Lemma 3.

Applying Lemma 3, we have

$$\Pr\{\Psi_{\tilde{\kappa}_{g,i}} > u'\} \geq 1 - O\left(\frac{1}{K'}\right) \quad (105)$$

where $\Psi_{\tilde{\kappa}_{g,i}} := \max\{\Psi_{g_1}, \dots, \Psi_{g_{K'}}\}$ and $u' = \lambda_{g,1} \log K' - \lambda_{g,1} \log \log K' + \lambda_{g,1} \log \frac{\zeta_{g,i}(\alpha, \epsilon)}{\xi_1}$.

Therefore, we obtain

$$1 - O\left(\frac{1}{K'}\right) \leq \Pr\{\Psi_{\tilde{\kappa}_{g,i}} > u'\} \stackrel{(a)}{\leq} \Pr\left\{\phi_{\tilde{\kappa}_{g,i}}^i > \frac{u'}{1/\rho + \epsilon}\right\} \quad (106)$$

$$\stackrel{(b)}{\leq} \Pr\{\phi_{\kappa_{g,i}}^i > u_g^i\}, \quad (107)$$

where $u_g^i = \frac{u'}{1/\rho + \epsilon}$ (see (52)). Here, (a) follows from the definition of Ψ_{g_k} and the inequality (101), and (b) follows from the fact that $\kappa_{g,i} = \arg \max \phi_{g_k}^i$. This concludes the proof. ■

Lemma 4: $\Pr \{ \|\mathbf{g}_{g_k}\|^2 \geq z \mid \mathbf{h}_{g_k} \in \overline{\mathcal{W}}_{g,i} \} > \Pr \{ \|\mathbf{g}_{g_k}\|^2 \geq z \}$.

Proof: Let $X := \lambda_{g,i} |\eta_{g_k,i}|^2$ and $Y := \sum_{m=1, m \neq i}^{r_g^*} \lambda_{g,m} |\eta_{g_k,m}|^2$. First, we represent the two events $\{\mathbf{h}_{g_k} \in \overline{\mathcal{W}}_{g,i}\}$ and $\{\|\mathbf{g}_{g_k}\|^2 \geq z\}$ in terms of X and Y . From (95), we have

$$\{\mathbf{h}_{g_k} \in \overline{\mathcal{W}}_{g,i}\} = \left\{ \frac{X}{X+Y} \geq \alpha^2 \right\} \quad (108)$$

$$= \left\{ X \geq \frac{\alpha^2}{1-\alpha^2} Y \right\} \quad (109)$$

$$= \left\{ X+Y \geq \frac{1}{1-\alpha^2} Y \right\}, \quad (110)$$

and $\{\|\mathbf{g}_{g_k}\|^2 \geq z\} = \{X+Y \geq z\}$. Thus, we have

$$\begin{aligned} & \Pr \{ \|\mathbf{g}_{g_k}\|^2 \geq z \mid \mathbf{h}_{g_k} \in \overline{\mathcal{W}}_{g,i} \} \\ &= \Pr \left\{ X+Y \geq z \mid X+Y \geq \frac{1}{1-\alpha^2} Y \right\} \\ &\stackrel{(a)}{=} \Pr \left\{ X+Y \geq z, Y \geq z(1-\alpha^2) \mid X+Y > \frac{1}{1-\alpha^2} Y \right\} + \Pr \left\{ X+Y \geq z, Y < z(1-\alpha^2) \mid X+Y > \frac{1}{1-\alpha^2} Y \right\} \\ &\stackrel{(b)}{=} \Pr \left\{ Y \geq z(1-\alpha^2) \mid X+Y > \frac{1}{1-\alpha^2} Y \right\} \cdot \Pr \left\{ X+Y \geq z \mid X+Y > \frac{1}{1-\alpha^2} Y, Y \geq z(1-\alpha^2) \right\} \\ &\quad + \Pr \left\{ Y < z(1-\alpha^2) \mid X+Y > \frac{1}{1-\alpha^2} Y \right\} \cdot \Pr \left\{ X+Y \geq z \mid X+Y > \frac{1}{1-\alpha^2} Y, Y < z(1-\alpha^2) \right\} \\ &\stackrel{(c)}{\geq} \Pr \left\{ Y \geq z(1-\alpha^2) \mid X+Y > \frac{1}{1-\alpha^2} Y \right\} + \Pr \left\{ Y < z(1-\alpha^2) \mid X+Y > \frac{1}{1-\alpha^2} Y \right\} \Pr \{ X+Y \geq z \} \\ &\stackrel{(d)}{\geq} \left[\Pr \left\{ Y \geq z(1-\alpha^2) \mid X+Y > \frac{1}{1-\alpha^2} Y \right\} + \Pr \left\{ Y < z(1-\alpha^2) \mid X+Y > \frac{1}{1-\alpha^2} Y \right\} \right] \Pr \{ X+Y \geq z \} \\ &= \Pr \{ X+Y \geq z \} = \Pr \{ \|\mathbf{g}_{g_k}\|^2 \geq z \}. \end{aligned}$$

Here, (a) follows from the law of total probability:

$$\Pr \{ A|C \} = \Pr \{ A, B|C \} + \Pr \{ A, B^c|C \}; \quad (111)$$

(b) holds by Bayes' rule; (c) follows from the fact that

$$\Pr \left\{ X+Y \geq z \mid X+Y > \frac{1}{1-\alpha^2} Y, Y \geq z(1-\alpha^2) \right\} = \Pr \{ X+Y \geq z \mid X+Y > z \} = 1 \quad (112)$$

and

$$\Pr\left\{X + Y \geq z \mid X + Y > \frac{1}{1-\alpha^2}Y, Y < z(1-\alpha^2)\right\} = \Pr\left\{X + Y \geq z \mid X + Y > z - \delta\right\} \quad (113)$$

$$= \frac{\Pr\{X + Y \geq z, X + Y > z - \delta\}}{\Pr\{X + Y > z - \delta\}} \quad (114)$$

$$= \frac{\Pr\{X + Y \geq z\}}{\Pr\{X + Y > z - \delta\}} \quad (115)$$

$$\geq \Pr\{X + Y \geq z\} \quad (116)$$

for some $\delta > 0$; and (d) is valid because the first term in the RHS is multiplied by $\Pr\{X + Y \geq z\} \leq 1$ from the previous step. ■

REFERENCES

- [1] G. Lee and Y. Sung, "Asymptotically optimal simple user scheduling for massive MIMO downlink with two-stage beamforming," submitted to 2014 *SPAWC*, Feb., 2014
- [2] G. Caire and S. Shamai, "On the achievable throughput of a multi-antenna Gaussian broadcast channel," *IEEE Trans. Inf. Theory*, vol. 49, no. 7, pp. 1691 - 1706, Jul. 2003
- [3] H. Weingarten, Y. Steinberg and S. Shamai, "The capacity region of the Gaussian MIMO broadcast channel," *Proc. of ISIT*, Chicago, IL, 2004
- [4] M. Sharif and B. Hassibi, "On the capacity of MIMO broadcast channels with partial side information," *IEEE Trans. Inf. Theory*, vol. 51, no. 2, pp. 506 -522, Feb. 2005
- [5] T. Yoo and A. Goldsmith, "On the optimality of multiantenna broadcast scheduling using zero-forcing beamforming," *IEEE J. Sel. Areas Commun.*, vol. 24, no. 3, pp. 528 - 541, Mar. 2006
- [6] M. Costa, "Writing on dirty paper," *IEEE Trans. Inf. Theory*, vol. 29, no. 3, pp. 439 - 441, May 1983
- [7] L. Liu, R. Chen, S. Geirhofer, K. Sayana, Z. Shi, and Y. Zhou, "Downlink MIMO in LTE-Advanced: SU-MIMO vs. MU-MIMO," *IEEE Commun. Mag.*, vol. 50, no. 2, pp. 140 -147, Feb. 2009
- [8] R. Knopp and P.A. Humblet, "Information capacity and power control in single cell multi-user communications," *Proc. Intl Conf. Comm.*, pp. 331-335, Seattle, WA, Jun. 1995
- [9] P. Viswanath, D. N. C. Tse, and R. Laroia, "Opportunistic beamforming using dumb antennas," *IEEE Trans. Inf. Theory*, vol. 48, no. 6, pp. 1277 - 1294, Jun. 2002
- [10] A. Adhikary, J. Nam, J. Ahn and G. Caire, "Joint spatial division and multiplexing: The large-scale array regime," *IEEE Trans. Inf. Theory*, vol. 59, no. 10, pp. 6441 - 6463, Oct. 2013
- [11] T. Al-Naffouri, M. Sharif and B. Hassibi, "How much does transmit correlation affect the sum-rate scaling of MIMO Gaussian broadcast channels?," *IEEE Trans. Commun.*, vol. 57, no. 2, pp. 562 -572, Feb. 2009
- [12] A. Adhikary and G. Caire, "Joint spatial division and multiplexing: Opportunistic beamforming and user grouping," *arXiv preprint arXiv:1305.7252*, 2013
- [13] M. Herdin and E. Bonek, "A MIMO correlation matrix based metric for characterizing non-stationarity," *Proc. the IST Mobile and Wireless Communications Summit*, Lyon, France, Jun. 2004
- [14] J. Hoydis, C. Hoek, T. Wild, and S. ten Brink, "Channel measurements for large antenna arrays," *Proc. IEEE ISWCS*, Paris, France, Aug. 2012

- [15] A. Ispas, M. Dörpinghaus, G. Ascheid, and T. Zemem, "Characterization of non-stationary channels using mismatched Wiener filtering," *IEEE Trans. Signal Process.*, vol. 64, no. 2, pp. 274 - 288, Jan. 2013
- [16] A. Ispas, C. Schneider, G. Ascheid, and R. Thomä, "Analysis of local quasi-stationarity regions in an urban macrocell scenario," *Proc. IEEE VTC*, Taipei, Taiwan, May 2010
- [17] S. Noh, M. D. Zoltowski, Y. Sung, and D. J. Love, "Pilot beam pattern design for channel estimation in massive MIMO systems," accepted to *IEEE J. Sel. Topics Signal Process.*, available at <http://arxiv.org/abs/1309.7430>, Dec., 2013
- [18] W. Jakes, *Microwave Mobile Communications*, Wiley, New York, 1974
- [19] D. Shiu, G. J. Foschini, M. J. Gans, and J. M. Kahn, "Fading correlation and its effect on the capacity of multi element antenna systems," *IEEE Trans. Commun.*, vol. 48, no. 3, pp. 502 - 513, Mar. 2000
- [20] T. Cover and J. Thomas, *Elements of Information Theory*, John Wiley & Sons, Inc., 1991
- [21] G. Dimic and N. D. Sidiropoulos, "On downlink beamforming with greedy user selection: Performance analysis and a simple new algorithm," *IEEE Trans. Signal Process.*, vol. 53, no. 10, pp. 3857 - 3868, Oct. 2005
- [22] C. B. Peel, B. M. Hochwald, and A. L. Swindlehurst, "A vector-perturbation technique for near-capacity multiantenna multiuser communication-part I: Channel inversion and regularization," *IEEE Trans. Commun.*, vol. 53, no. 1, pp. 195 - 202, Jan. 2005
- [23] R. A. Horn and C. R. Johnson, *Matrix Analysis*, Cambridge University Press, Cambridge, UK, 1985
- [24] Y. Huang and B. Rao, "Random beamforming with heterogeneous users and selective feedback: Individual sum rate and individual scaling laws," *IEEE Trans. Wireless Commun.*, vol. 12, no. 5, pp. 2080 - 2090, May 2013
- [25] S. Boyd and L. Vandenberghe, *Convex Optimization*, Cambridge University Press, New York, NY, 2004
- [26] H. A. David and H. N. Nagaraja, *Order Statistics*, John Wiley & Sons Inc., New York, 2003
- [27] N. V. Smirnov, "Limit distributions for the terms of a variational series," *Trudy Mat. Inst.*, vol. 25, 1949
- [28] E. Castillo, *Extreme Value Theory in Engineering*, Academic Press, Inc., San Diego, CA, 1988
- [29] M. A. Maddah-Ali, M. A. Sadrabadi, and A. K. Khandani, "Broadcast in MIMO systems based on a generalized QR decomposition: Signaling and performance analysis," *IEEE Trans. Inf. Theory*, vol. 54, no. 3, pp. 1124 - 1138, Mar. 2008
- [30] D. Hammarwall, M. Bengtsson, and B. Ottersten, "Acquiring partial CSI for spatially selective transmission by instantaneous channel norm feedback," *IEEE Trans. Signal Process.*, vol. 56, no. 3, pp. 1188 - 1204, Mar. 2008